MANUFACTURING AND CHARACTERIZATION OF A 3D-PRINTABLE, ANTIBACTERIAL, MAGNESIUM OXIDE NANOPARTICLES REINFORCED ABS FILAMENT

by

Saket Thapliyal

Presented to the faculty of graduate school of

The University of Texas at Arlington, in partial fulfillment of the requirements for the degree of

Master of Science in Mechanical Engineering

The University of Texas at Arlington

Thesis committee:

Dr. Ashfaq Adnan, Chair

Dr. Wen S Chan

Dr. Robert Taylor

April, 2017.

UNIVERSITY OF
TEXAS
ARLINGTON

ABSTRACT

This research work consists of two phases. In phase one it is intended to manufacture an antibacterial 3D printable filament by extruding a solid state mixture of (MgO) nanoparticles (NPs) and Acrylonitrile Butadiene Styrene (ABS) pellets. A single screw extruder was used to extrude ABS pellets containing 0, 0.5, 1, 2 and 4 wt. % MgO NP. This phase deals with manufacturing and testing the filament for mechanical properties, antibacterial properties and 3D printability. On one hand tensile strength, ductility and 3D-printabiliy were observed to decrease with increasing concentrations of MgO NP in ABS matrix, on the other hand the extent of inhibition of microorganisms was found to increase with increasing concentration of NP. Moreover, diametric inconsistency of the extruded filaments was observed to increase with increasing NP concentrations. The 4 % filament was unprintable for the Fused Deposition Modelling (FDM) printer while the 2 % filament required several attempts in order to be 3D printed. A concentration of 0.5 wt. % of MgO inhibited the growth of *Bacillus subtilis*, whereas the filaments having 1 and 2 wt. % of MgO inhibited the growth of *Klebsiella* pneumoniae and Pseudomonas aeruginosa. The filament having no MgO NP did not exhibit antibacterial activity.

Phase two of this research deals with determination of factors that decide the mechanical properties and 3D printability of ABS-MgO nanocomposite filament. Moisture in the hygroscopic MgO NPs (ILO-ICSC, 2010) was believed to be the reason for generation of voids therefore bringing about deterioration of mechanical properties and 3D printability of the nanocomposite filaments. The filament containing maximum w/w concentration (2%) of non-heated MgO NPs in unground ABS pellets was found to contain voids of largest average size and lowest average tensile strength; however, when a similar concentration mixture of 2% MgO in ABS (w/w) was made from heat dried MgO NPs and ground ABS pellets and then extruded, the average size of void inside the filament decreased by more than 90 % and the average ultimate tensile strength (UTS) of the filament increased by more than 84 %. Furthermore it was possible to 3D print the 2% filament containing ground ABS pellets and heat dried MgO NPs in a single iteration. These results indicate that pre-conditioning of the pellets and NPs is a deciding factor in preventing the deterioration of properties of an extruded nanocomposite material. With improved mechanical properties and 3D printability the two-step manufacturing method can be used to build smart objects that apart from bearing load would have antibacterial bacterial properties intrinsic to them.

ACKNOWLEDGEMENT

Sharing knowledge and perspectives to understand science, learning the art of manufacturing functional structures and witnessing extremely small dimensions of nature and its phenomena have fuelled my zest to observe and build, but none of these fortunes would have come my way without the fortune of having Dr. Ashfaq Adnan as my advisor. He helped me in every possible manner right from giving his time for mentoring and discussions to providing the facilities and equipment that were needed for this research, arranging financial support and encouraging me to keep going. I'm most grateful to him for providing the comfortable environment where thoughts and perspectives could flow freely and where I was trusted. I wish to thank him from the depth of my heart for elucidating the lines between 'the subjective' and 'the objective' in science.

I'm extremely thankful to Dr. Kevin A. Schug and his team including Dr. Inês C. Santos and Misty S. Martin from the Department of Chemistry and Biochemistry at University of Texas, Arlington (UTA), for collaborating with us and performing antibacterial tests which added a very important dimension to my research. I'm also thankful to Dr. Jiechao Jiang and Dr. Efstathios I. Meletis for allowing me to use the Characterization Center for Materials & Biology (CCMB) facility at the UTA. I wish to thank Dr. Wen S. Chan and Dr. Robert M. Taylor for giving their valuable time to me and for being in my committee. I'm thankful to the graduate advisor at the department of mechanical engineering (ME) at the UTA, Dr. Seiichi Nomura for being accessible whenever needed and for his profound advising. I'm also grateful to the administrative and technical staff at the ME department including Debi Barton, Lanie Gordon, Flora Pinegar, Catherine Gruebbel, Ayesha Fatima, Mike Baker and Kermit Beird for their assistance.

I extend a special thanks to my colleagues Dr. Yuan T. Wu, Dr. Peter LeBoulluec, Dr. Fahad Ferdous, Fuad Hasan, Riaz Kaiser, Amit Khatri, Hassan Mahmud, Blesson Isaac, Rajni Chahal, Ishak Khan, Krutarth Patel and Megha Tangri for their support and suggestions. Last but foremost, I'm blessed to have the support of my parents and family in times of joy as well as despair. I'm grateful to them for inspiring me, being a driving force in my life, for teaching me values and the strength of love.

April 18, 2017.

PREFACE

Despite accelerated growth in 3D printing technologies for developing novel structures, technological advances in developing multifunctional structures using 3D printing is yet to be achieved. Here, the process of polymer extrusion is utilized to build a multifunctional (antibacterial and structural) 3D-printable filament from solid state mixture of magnesium oxide nanoparticles and ABS pellets. The need for developing such multifunctional structure is underscored by World Health Organization (WHO)'s prediction that deaths due to infectious diseases could reach to 13 million even in 2050. It is believed that through this cost effective, two-step process of extrusion followed by 3D printing, infusion of antibacterial properties in plastics used in common household items such as furniture and toys, electronic equipment such as smartphones, tablets, computer keyboards and other electronic healthcare equipment, on which a diverse bacterial environment exists, would greatly reduce the risks of acquiring bacterial infections. The first phase of the study involves developing a customized extrusion method to develop 3D printable nanocomposite filaments. In the next phase, the antibacterial and structural performance of the filaments and 3D printed structure was measured. It was found that with the increase in w/w concentration of MgO NPs, the bacterial inhibition increased whereas the mechanical properties and 3D-printabilty decreased. Factors that decide the mechanical properties and 3D printability of ABS-MgO nanocomposite filament were determined. SEM micrographs showed presence of closely spaced voids in the nanocomposite filaments. Preconditioning of the mixture constituents significantly improved the 3D printability and mechanical properties of the nanocomposite filament.

Table of Contents

LIST OF FIGURES AND TABLES:

1. INTRODUCTION:

Besides being a driving force for life, nature has always been a motivational force for researchers and scientists (Dunlop and Fratzl, 2015) (Guo, Gao, 2006), (Wegst et al.,2015) its systems might look very simple but they can be as intricately engineered as human skin (Cohen, 2005 (310)). The system of heterogeneous materials exists with stability in nature and such systems are known to possess marvellous amounts of multi-functionality. These systems have inspired researchers to understand the importance of heterogeneity because it brings about smartness and multifunctionality in the materials. Nature uses heterogeneity in its structures and materials in a prominent manner from bones to skin. Although these naturally occurring structures are functional in different aspects such as load bearing, transport and storage of nutrients and minerals (McDowell et al.; 42) they do not exhibit similar mechanical properties when exposed to different conditions such as radiation (Suva and Griffin, 2012). Another example of trade-off between properties in natural materials is the mutual exclusiveness of strength and ductility which in order to be inclusive within a material requires changes in structure and constituents (Zhu et al., 2015). One such heterogeneous but man made material is plastic which along with being light weighted and strong, is relatively easier to process. From toys to critical medical equipment, we are surrounded by plastics and thus they have certainly become materials of great importance to us.

Plastics are extensively used in a broad range of applications such as construction, home goods, electronics, sports, toys and aerospace industries. Wide range of desired properties such as excellent strength to weight ratio, durability, cost effectiveness, ease of processing, low maintenance, corrosion resistance as well as versatility make plastics economically attractive and materials of choice. Moreover the revolutionary emergence of additive manufacturing technology has further added to the popularity and ubiquity of plastics.

A study by Hirsch et al. (2014) showed that electronics used in healthcare system can harbour both gram positive and gram negative bacteria. Dunn et al. (2013) conducted a similar study for household environment whereas Peleg et al. (2010) and Poza et al. (2012) conducted a study to find out bacterial diversity in hospitals. Davies et al. (2000) and buttery et al. (1998) studied bacterial diversity on toys used in neonatal settings. Another study conducted by Klaus et al. (2006) talked about bacterial diversity in spacecraft during flight.

Presence of bacteria such as *Klebsiella pneumoniae, Pseudomonas aeruginosa, Staphylococcus aureus* etc. was reported in these environments. Usage of plastics is popular in these diverse scenarios ranging from household and hospital environments to public transport (Otter et al.) and aerospace. Infectious diseases still cause a large amount of deaths worldwide (Dye, 2014). The World Health Organization (WHO) has predicted that in 2050, 13 million deaths will be caused by infectious diseases (Fig. 1). Moreover, antimicrobial resistance is growing among bacteria (Ventola et al., 2015), (Garbati et al., 2013), (Cabot et al.). WHO recently published a list of twelve bacteria, that are resistant to multiple drugs (WHO, 2017) and for which new and effective treatments are desperately needed. It is believed that introducing antibacterial properties in plastic objects used in common household items such as furniture and toys, electronic equipment such as smartphones, tablets, computer keyboards and other electronic healthcare equipment, on which a diverse bacterial environment exists, would greatly reduce the risks of acquiring bacterial infections.

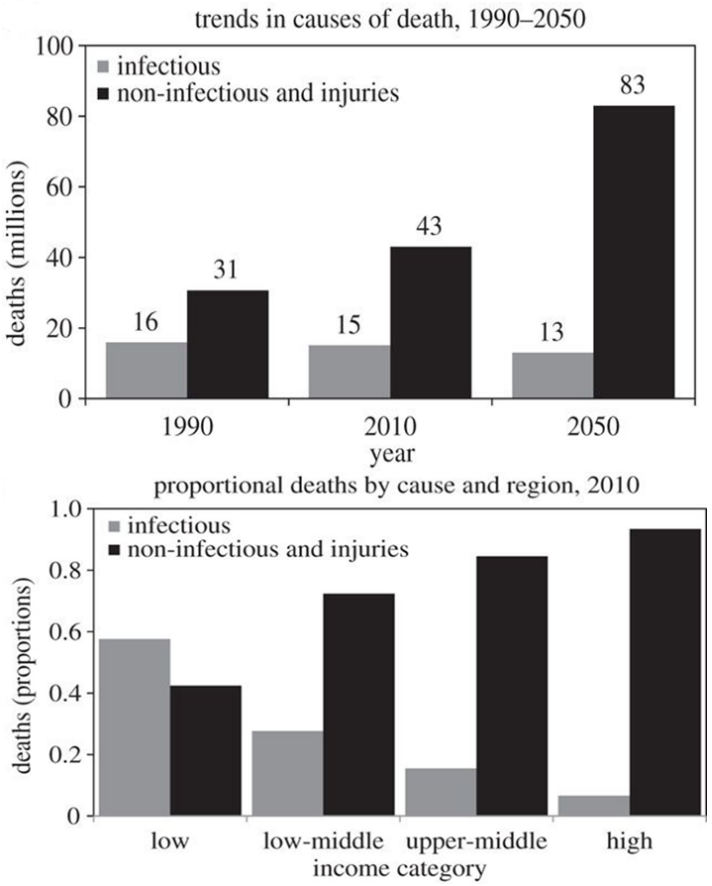

Figure 1: Top: Trends in infectious and non-infectious related deaths between 1990 and 2050. Infectious diseases include maternal and nutritional disorders whereas non-infectious diseases include injuries. **Bottom:** Proportional deaths due to infectious and non-infectious diseases among different income groups and regions.

Antibacterial coatings are a popular method of resisting bacterial pathogens (Coultier et al.) but these coatings can get rubbed off from the surface of the object over the course of time due to friction. Moreover, these coatings often need to be synthesized in a different facility than the object and oftentimes require a treatment facility to coat them on object thus increasing costs. With the emergence of additive manufacturing, processes of manufacturing have been simplified. The popularity and ease of accessibility of 3D-printers have made it possible for the end users to manufacture and build at home. Furthermore, it is possible to alter the composition of polymers and add functionalities to them and thanks to additive manufacturing, these multifunctional plastic objects need not be built in specialised manufacturing facilities. In order to add functionality in objects around us we just need to build a 3D printable functional filament, e.g., Goh et al. (2015) built a conductive filament and proposed that circuit board can be built at home faster than the conventional fabrication processes of etching and soldering at a cheaper price. Mahfuz et al. (2007) built a Silica NPs-Nylon 6 nanocomposite filament through melt-extrusion to improve mechanical properties of nylon filament. Although, 3D printing was introduced in 1980s, diversity in types of functional filaments is yet to be achieved and aesthetics of the printed product still remain an issue for filament manufacturing industry. In this research, an attempt has been made to use a two-step process of extrusion followed by 3D printing to build a functional 3D-printable filament. It is believed that this 2 step process can greatly diversify the types of functional filaments available in the market today.

First phase of this work has been targeted to add functionality such as antibacterial activity to ABS which is often used in children's toys, medical devices, electronic appliances, aerospace, defense and automotive industries. The antibacterial property is added by infusing MgO NPs in the ABS matrix using the process of polymer extrusion. NPs are gaining popularity as antimicrobial agents that can inhibit multiple drug resistant bacteria (Pelegrift et al. (2013)), (Tillotson et al. (2013)), (Zhang et al. (2010)), (Beyth et al. (2015)). MgO is known to exhibit antibacterial properties against some harmful bacteria such as Klebsiella *spp*. and *Pseudomonas Aeruginosa* (Gokulakrishnan et al., 2012). Moreover, it has also been found that decreasing particle size results in increasing antibacterial activity in MgO (Lei et al., 2005), (Jin et al., 2011) and MgO does not pose a long term health hazard (Hazardous Substance Fact Sheet) therefore MgO NPs were used as antibacterial agents. The idea of this research is to determine whether or not it is possible to add multifunctionality to a polymer using a cost effective and easily accessible technology of plastic extrusion and then to process that polymer using 3D printing. If it becomes feasible to add functionality in ABS by a

certain technique, then functionality can be achieved in other polymer using the same technique. It is desired to add anti-bacterial properties to ABS by addition of NPs using a two-step process of extrusion and 3D printing. A solid mixture of ABS pellets and MgO nanoparticles at different concentrations was fed into a single screw extruder that extrudes a 3D printable filament under set of controlled conditions discussed in appendix. The prepared samples were able to inhibit bacteria such as *Pseudomonas aeruginosa*, *Klebsiella pneumoniae* and *Bacillus subtilis* that are known to resist antibiotics (Slama, 2008). Although the extent of inhibition of bacteria was observed to increase with increasing NP concentration in ABS, deterioration in strength, ductility and 3D-printability was also observed with increasing NP concentration. When nanocomposite filaments containing 4, 2, 1 and 0.5 wt. % MgO NPs were tested for 3D printability, the printer extruder stopped extruding the 4% filament after some time while it took 3 iterations for printing the 2% filament whereas 1% and 0.5% filaments were successfully 3D printed in the first attempt.

In second phase of this research work, factors that control the mechanical properties and 3D printability were determined by analysing filament samples containing different concentrations of MgO NPs for void size under Scanning Electron Microscope (SEM) and diametric consistency. Formation of voids and bubbles at higher NP concentrations was considered to be the reason behind deteriorating 3D printability with increasing concentration of NPs inside the polymer matrix. Voids or bubbles inside or on the extrudate surface might be formed due to presence of volatile impurities (moisture) in the mixture (Giles, Wagner (401)). Being hygroscopic in nature, MgO NPs were believed to cause formation of bubbles and voids on the surface and inside the nanocomposite filament. Diametric errors of up to ±0.25 mm and ±0.42 mm were observed in 2% and 4% filament respectively from the expected value of 1.75 mm. The bubbles formed on the surface and inside the filament were observed to adversely affect diametric consistency and roundness which in turn might make gripping of the filament difficult for the gripping gears of 3D printer extruder and thus making the nanocomposite filament poorly compatible with the in house FDM type printer. Moreover, the tensile strength of filament with 2 wt. % MgO was observed to decrease by more than 51% when compared to the supplied pure ABS filament. Voids were also believed to be the main reason behind deteriorating mechanical properties of the nanocomposite filaments (Anderson et al., 2014) with increasing NP concentration**.** Sudheer et al. (2014) reported that strength and fracture strain decreases with increasing loading of potassium titanate whisker (PTW). Hwang et al (2015) reported that when copper and iron particles were added in ABS matrix to obtain thermally conductive 3D printable filament as the tensile

strength and ductility were found to decrease, the thermal conductivity was observed to increase with increasing metal particle concentration in polymer matrix. At first it is desired to validate the hypothesis that volatile impurities in the mixture constituents affect tensile strength and diametric consistency of the extrudate (where diametric consistency is directly related to 3D printability of the filament) as it brings about generation of voids and bubbles inside and on the surface of the nanocomposite filament. Secondly, determination of processing and pre-conditioning methods is done which can inhibit the deterioration of mechanical properties and 3D printability when NPs are added to the polymer matrix via the process of polymer extrusion. It was believed that pre-conditioning methods that can facilitate removal of moisture from the mixture and other volatile impurities or irregularities such as air bubbles from the melt pool will prevent deterioration of properties of nanocomposite filament. Although this research only deals with pre-conditioning of MgO NPs and ABS for synthesis of their nanocomposite, the methods discussed can be used for pre-conditioning of other polymers and hygroscopic NPs for synthesizing a different nanocomposite material. The unconditioned filament was found to inhibit both gram positive and gram negative bacteria and since several mechanisms of antibacterial action of MgO NPs are known (Tang et al., 2014) therefore it is believed that the antibacterial properties of the nanocomposite filament would not deteriorate with pre-conditioning of its matrix and reinforcement and thus no further antibacterial tests were performed on the filament.

With deteriorated mechanical properties this antibacterial nanocomposite material can only be useful in building items that usually do not bear a lot of load such as toys, fragile healthcare equipment, etc. but with improved mechanical properties this material has potential area of application in aerospace and places where it is not possible to practice conventional methods of inhibiting bacteria.

With this filament, it is possible to manufacture objects having antibacterial properties intrinsically using a 3D printer; this can possibly eliminate the need for treatment of objects with antibacterial agents or coatings. This research work should be apprehended as an attempt to introduce multifunctionality in objects or structures around us by using a technology that does not require large space, large investment or specialised manufacturing expertise. Such filaments can be used for building very affordable anti-bacterial plastic toys that would probably make parents less worried about the health risks associated with toys, noting the microbial environment that is found to exist on them (Stauber et al., 2013), (Bastidas et al.) other uses would be to build products used in hospitals and healthcare, electronics and

furniture industry, public transport and aerospace where conventional methods of inhibiting bacteria are difficult to practise.

2. MATERIALS AND APPARATUSES:

2.1. Magnesium oxide nanoparticles

20 nm (average particle size) MgO nanoparticles, purchased from Nanostructured & Amorphous Materials Inc. have been used in this experiment to achieve antimicrobial properties.

2.2. Acrylonitrile Butadiene Styrene (ABS) pellets

ABS in pellets form was purchased from Revolve3d. The manufacturer recommended extrusion temperature for these pellets is 180-190°C and the pellets can provide extrusion rate of 4-15 inches per minute. The dimension of purchased pellets was such that the longest side for most of the pellets did not measure more than 5 mm.

2.3. Filament extruder and winder

A single screw, bench-top extruder and a filament winder purchased from Printit industries have been used. The mentioned extrusion rate is 12-18 in/min with MG94 ABS. The extruder and filament winder were customized in the laboratory. As shown in Fig. 2, a hopper, hopper cover, spacer for the winder unit and a tripod stand for the winder shaft were designed and 3D printed to integrate with the original extruder. A filament winder (Fig. 2A) winds the extruded filament on a spool and has 2 modes of operation: manual and automatic winding. The supply current in the unit was maintained in the range 1.4-1.6 amp and the voltage to 12 Volts. A Proportional-Integral-Derivative (PID) controller is used to build filament with 1.75 mm nominal diameter. In order to achieve consistent diameters of the extruded filament, an effective cooling mechanism for the hot extruded filament was added. This is necessary because the extruded filaments must be cooled rapidly below its glass transition temperature so that desired size and shape could be maintained (Giles, Wagner, Mount (9)). Air cooled system was implemented and air fan that came with the extruder (rated at 12 V & .16 A) was replaced with a more powerful Thermaltake CPU fan (rated at 12 V & .20 A). To dampen vibrations in the replacement fan, it was firmly fixed between a

wooden block and shelf floor using clamps (Fig 2B). More details about the set-up and parameters controlled to obtain a 3D printable filament are provided in the appendix.

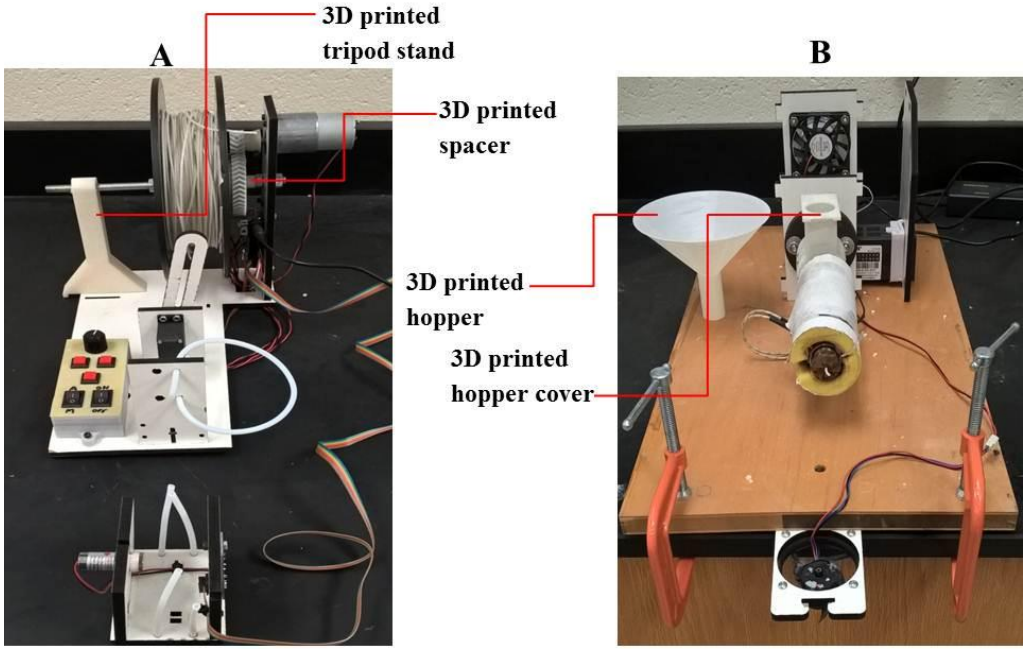

Figure 2: Lab assembled Filament winder (A) and filament extruder (B)

2.4. 3D-printer

The Makerbot Replicator 2X Fused Deposition Modeling (FDM) type 3D printer was used for all 3D printing jobs carried out during the experiment. To control print parameters in the specimens such as infill percent, nozzle and bed temperature, Makerbot Desktop software was used.

2.5. Mechanical Tester

Shimadzu AGS-X mechanical tester was used for all the tensile testing jobs carried during the experiment. Load on this machine can reach a maximum limit of 10 KN.

2.6. Apparatuses for antibacterial testing

The antibacterial properties of the filaments were tested against *Acinetobacter baumannii* ATCC 19609, *Bacillus subtilis*, *Escherichia coli* ATCC 25922, *Klebsiella pneumoniae* ATCC 13883, and *Pseudomonas aeruginosa*. Nutrient agar and nutrient broth (NA and NB, Sigma-Aldrich, St. Louis, MO, USA) were prepared according to supplier's protocol and used to grow and maintain bacterial cultures.

2.7. Oven

An in-house convection oven from Oster was used to heat the NPs so as to remove the volatile impurities from the NPs. Maximum achievable temperature inside the oven is 232.2 °C. Since MgO is known to be a hygroscopic solid, it was intended to heat the NPs.

2.8. Burr grinder

An in-house wheel burr grinder GX6000 from Krups was used to grind the ABS pellets. It was desired to reduce the pellet size so as to curb the adverse effects of moisture on the dimensional consistency of extrudate and to facilitate better mixing of pellets with NPs (section 3.1). User can chose from different available coarseness settings in the grinder. The ABS pellets in this experiment were ground at the finest setting. Burr grinder was preferred over blade grinder because of its ability to crush the coffee beans between a rotating wheel and a stationary surface unlike blade grinder which chops the beans with blades; moreover burr grinder produces more consistently sized particles and is known to produce lesser heat in comparison to the blade grinder. It is believed that cryogenic grinding would have produced finer particle size but was not used because of high setup costs.

2.9. Scanning Electron Microscope (SEM)

Hitachi S-3000N variable pressure SEM (VP-SEM) available at University of Texas, Arlington was used throughout this experiment to determine the void size of differently pre-conditioned filament samples. Pure ABS and nanocomposite filament samples were sputtered with silver NPs to be analysed under high vacuum mode.

3. EXPERIMENTAL METHODOLOGY:

3.1. Methods used in first phase:

Methodology in phase one is concerned with tuning the apparatus for manufacturing the nanocomposite filament, mechanical testing and characterization of the filament and testing the filament for 3D printability.

3.1.1 Preparation of ABS-MgO mixture

Antibacterial properties of MgO are directly dependent on concentration and size of MgO NP. It was thus desired to add MgO NP in ABS pellets at higher concentrations. ABS-MgO mixtures having MgO 0.5%, 1%, 2% and 4% (w/w) were prepared by sprinkling NP over ABS pellets followed by through shaking of the mixture.

3.1.2 Extrusion:

Pure ABS or ABS-MgO mixture was fed into the extruder via hopper. For pure ABS, the processing temperature was set to 185°C on temperature controller; for 0.5 and 1 wt. % mixture of MgO the temperature was set to 190°C whereas for mixtures containing 2% and 4% MgO, the temperature was set to 195°C. Details on temperature selection are provided in appendix. At first a sample ABS filament containing no MgO NP was extruded and then other 4 types of sample filaments, containing 0.5 %, 1% , 2% and 4% (all in w/w) MgO NP, were extruded. Before feeding the extruder with a different mixture having certain concentration of MgO, extruder was each time fed with pure ABS and was run until a completely round to feel filament having no air bubbles (which indicate no or negligible MgO NP on the filament surface) was obtained. Extruded filament was collected on a clean mat which lies 3 ft. below the nozzle. After a desired length of filament was extruded, it was coiled onto the spool using filament winder.

Sample filaments of length 10 ft. from each category were inspected for diameter at 12 equidistant locations. Root mean square error (RMSE) for all the filament types was calculated using the expected diameter of 1.75 mm as mean value.

$$RMSD = \sqrt{\frac{1}{n}\sum_{i=1}^{n}(D_{o(i)} - D_{e(i)})^2}$$

Where: $\boldsymbol{D_o}$ is obtained diameter

$\boldsymbol{D_e}$ is expected diameter (1.75 mm)

$\boldsymbol{n}$ is number of readings

$(D_{o(i)} - D_{e(i)})$ is the diametric error (in mm)

The RMSE values increased with increasing concentration of MgO NPs in the ABS matrix. Besides having diametric errors of up to ±0.46 mm, the 4% filament was observed to have poor roundness and surface finish. This filament had bubbles bulging out of the surface

and when cut along its length, voids were visible to the unaided eye however when pure ABS filament was observed in a similar way, no voids were visible (Fig. 3A and 3B**)**. Fig. 4 shows variation of diameters in 4 samples of different types of filament. Lowest diametric error of ±0.04 mm from expected value of 1.75 mm was obtained from pure ABS filaments. The extruded filaments (pure ABS and nanocomposite filaments) were then checked for 3D printability. The printer nozzle and platform temperatures were set to 230°C and 110°C and the infill was set to 25%. The manufacturer recommended filament diametric tolerance for in house 3D printer (for the filament to be 3D-printable) is ±0.10 mm while from experiments it was observed that the tolerance could go up to ±0.15 mm; due to poor consistencies of the 4% filament, it could not be 3D printed. Since it is intended to produce a 3D printable antibacterial nanocomposite filament, filament containing 4% MgO NP (w/w %) was not included among samples for mechanical and antibacterial testing. Although the 2 % filament samples were also found to have high diametric error of up to ±0.22 mm, few of the filament sections had errors within ±0.15 mm and thus these sections were observed to be 3D printable.

Figure 3: Cross sectional view of pure ABS filament sample having no visible voids (A) and of filament with 4 wt. % MgO having visible voids (B)

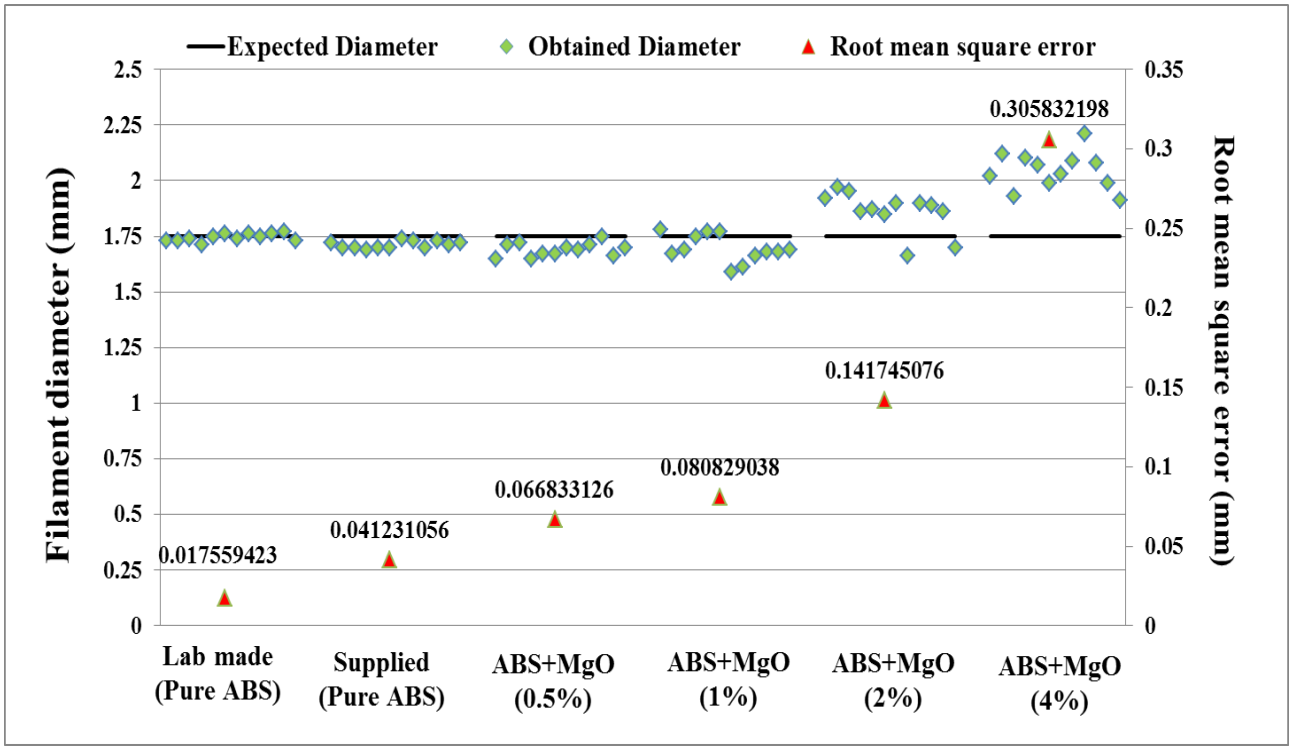

Figure 4: Comparison of diametric consistencies for filaments having different NP concentrations

3.1.3 Mechanical testing of filaments

Samples of filament of length 10 cm between grips and from each concentration category i.e. 0%, 0.5%, 1% and 2% w/w MgO (all extruded using the in house extruding apparatus) were tensile tested using the mechanical tester and the results were compared to those obtained from testing of supplied pure ABS filament. The loading rate was set at 2 N/s and during trial runs the filament samples (especially the nanocomposite filaments) were observed to be breaking frequently near the grips. However, when filament ends were tape wrapped 4-5 times with a fabric reinforced adhesive tape so as to prevent undue stress concentration on filament ends, the samples failed less frequently near the gips. The mechanical properties of filaments that did not fail near the grips have been reported in this research.

3.1.4 Antibacterial testing of nanoparticles

B. subtilis, *E. coli*, and *K. pneumoniae* were grown in the presence of MgO NP in order to determine the antibacterial properties of the NP. Initially, *B. subtilis*, *E. coli*, and *K. pneumoniae* were grown overnight in NB at 37ºC. NA was prepared according to manufacturer's protocol and allowed to cool to 50ºC. MgO NP were added to the NA to make

a final concentration of 1 w.t. %. The media containing the nanoparticles was plated and allowed to solidify. Cultures previously grown overnight were inoculated on NA containing the MgO nanoparticles, directly from the NB, spreading the inoculum as evenly as possible. Plates were incubated at 37ºC overnight. The bacteria were also grown on NA as a control. Bacterial growth was observed by visually inspecting the opacity of the plates.

3.1.5 Antibacterial testing of filaments

Disc diffusion method for antibacterial susceptibility testing was performed using the standard method (Bauer *et al*., 1966) in order to assess the presence of antibacterial activity of the prepared filaments at different concentrations of MgO (0, 0.5, 1, and 2 w.t. %). *A. baumannii, B. subtilis, E. coli, K. pneumoniae*, and *P. aeruginosa* were grown overnight in NB at 37ºC. Cultures were inoculated on to NA directly from the suspension, spreading the inoculum as evenly as possible. Three mm long filaments were placed with the aid of sterile tweezers to the inoculated medium. Each filament concentration was tested in triplicates. Plates were incubated at 37ºC overnight. The diameters of the inhibition zones surrounding the filaments were measured in millimetres. This assay was repeated once more to ensure reproducibility.

3.2. Methods used in second phase:

The antibacterial testing, mechanical testing and test for 3D printability of pure ABS and nanocomposite filaments containing 0, 0.5, 1, and 2 wt. % MgO NPs mark the end of phase one of this research. Methodology in phase two is concerned with determination of parameters that control the properties of nanocomposite filament and validating the findings by further testing. Since the filament containing 2 wt. % MgO NPs was found to inhibit bacteria to the greatest extent but was observed to have least UTS among other 3D printable filaments, therefore only 2 % filament was processed and tested in this phase; the obtained properties of this filament were then compared with those of pure ABS filament

3.2.1 Pre-conditioning of Pellets and NPs

ABS pellets were ground to increase the overall surface area of the pellets available for conduction melting inside the barrel. It was believed that grinding the pellets would increase heat transfer (Chung, 2011(29)), facilitating improved flow of mixture due to decreased melt viscosity within the barrel. As the volatile impurities such as moisture, exit the extruder nozzle with the melt, they tend to expand and form bubbles and voids on and

inside the filament surface. Decreased melt viscosity would offer less resistance to bubble expansion and would allow them to rupture and escape from filament surface as the molten mixture exits the nozzle (Giles, Wagner, Mount, P 603) thus removing volatile impurities from the melt pool. Another method of reducing the melt pool viscosity is by setting a higher barrel heater temperature. Barrel heating only contributes 10-20% of the total heat required to melt the polymer (Giles, Wagner, Mount, P 53) and it does not ensure greater surface area of pellets and better conduction melting. Reduced viscosity would also reduce the extruder motor load (Sorroche et al., 2013) (Gupta et al., 2016) and thus would prevent abrupt stopping of extruder motor which was frequently observed to stop while extruding filaments having high MgO NP concentration. Furthermore, the ground pellets were observed to have static charge on them because of which, the sprinkled NPs had a tendency to stick to the ground pellets. This was believed to be useful in preventing the segregation of NPs from the pellets which is generally observed if there is a large size difference between constituents of a mixture (Giles, Wagner, Mount; 49). The prevention of segregation is likely to cause more uniform dispersion of NPs within the molten ABS and thus may improve antibacterial properties of the filament.

Pre-conditioning of NPs was done with an intention to reduce moisture content which was believed to be the reason for generation of voids and bubbles within and on the surface of the nanocomposite filament. NPs were heated inside a glass beaker kept inverted within the oven. The NPs were kept and spread over an aluminium foil. Opening of inverted glass beaker was then kept on the foil and the outlying foil edges were wrapped around the circumference of the beaker opening (Fig. 5). Inside the oven, NPs were kept on aluminium foil rather than on glass beaker because of high thermal conductivity of aluminium than glass. Initially NPs were weighed and then heated at 204.44 °C (400 °F) to check for the presence of volatile impurities. A loss of 7.14 % in weight was recorded after heating NPs for about 90 minutes which indicates presence of volatile impurities within the non-heated NPs. Prior to mixing with ground pellets required weight of NPs was heated at 204.44 °C for about 90 minutes. NPs were then sprinkled over ground ABS pellets and then the mixture was thoroughly shaken before feeding it into extruder hopper. Table 1 shows the nomenclature used for filaments containing 2 wt. % MgO NPs with differently pre-conditioned constituents.

Pre-conditioning method used	Nomenclature used for filament
Non heated NPs + Unground pellets	Type 1
Heat dried NPs + Unground pellets	Type 2
Non heated NPs + Ground pellets	Type 3
Heat dried NPs + Ground pellets	Type 4

Table 1: Nomenclatures for multifunctional filaments made from differently pre-conditioned constituents (all filaments contain 2 wt. % of MgO NPs.

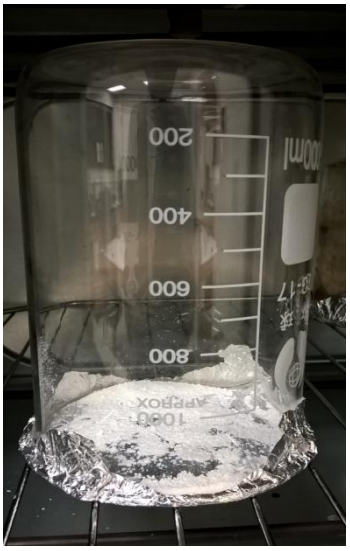

Figure 5: Setup for heat drying NPs inside oven

3.2.2 Extrusion

Pure ABS pellets and ABS-MgO mixtures containing 2 wt. % MgO NPs were fed into the extruder and were extruded at 185°C and 195°C respectively to produce filament of diameter 1.75 mm. Prior to producing a different type of filament, the extruder was flushed with pure ABS pellets until a completely round to feel filament containing no air bubbles (indicating no or negligible traces of MgO NPs) on filament surface and a round to feel filament was observed. Pure ABS or the nanocomposite filament was extruded using extruder and then was collected on a clean mat lying 3 feet below the extruder nozzle. The filament was then wound on the spool revolving on shaft of the filament winder. The filament samples were inspected for diametric consistency which is believed to directly affect the 3D printability of a filament. Filaments of each type were inspected for diameters at 12 different locations at an interval of 10 in. Pure ABS filaments were expected to have better consistency; RMSE of each filament type was determined using the diameter of 1.75 mm as expected value and the consistencies of 4 types of filaments (Table 1) were then compared with that of pure ABS filaments.

3.2.3 Microscopic analysis and Mechanical testing

Mechanical testing of all type of filaments was done using Shimadzu AGS-X universal tester at a loading rate of 2N/s. Four sample filaments from all filament types were cut such that all the samples measured 10 cm between the tester grips. The stress-strain response of the different filaments was compared.

In order to validate the hypotheses that voids and bubbles generated due to moisture not only affect the tensile strength of MgO-ABS filament but also its diametric consistency, pure ABS filament and all other filament types shown in Table 1 were analysed under VP-SEM for determination of void size. It was also desired to compare void sizes for differently pre-conditioned filaments and pure ABS filaments. Sample filaments of length 1 cm from each category were cut along their lengths and then sputter coated with silver. Secondary Electrons (SE) detector was used on high vacuum mode and accelerating voltage was set to 25 kV.

Filaments made of different combinations of conditioned constituents were tested and analysed to understand which of the conditioning method was most effective in making strongest and most diametric consistent filament.

3.2.4 Test for 3D printability

After comparison of diametric consistencies was done, it was desired to inspect the strongest and most diametric consistent filament type for 3D printability using the in-house FDM printer. The temperature of printer nozzle and platform was set to 230°C and 110°C respectively and the infill level was set to 25 %.

NOTE: Antibacterial tests were not performed in this phase because MgO NPs are known to have several antibacterial mechanisms few of which are listed below:

- Electrostatic forces between bacteria and MgO NPs (Hamouda et al., 2000).
- Alkalinity of MgO (Sawai et al., 2001; Yamamoto et al., 2000).
- MgO NPs produce superoxide ion (O2-) which damages cell wall (Huang et al., 2005; Lin et al. 2005; Yamamoto et al., 2010; Yamamoto et al., 2001).
- Being hygroscopic in nature, MgO adsorbs water which results in high pH value thus destroying bacterial cell membrane (Sawai et al., 1997).

Even though NPs were heat dried, it is believed that they would still adsorb water when they are present in the 3D printed object and therefore heat drying NPs is not believed to be hampering the antibacterial mechanism. The antibacterial properties may in fact improve due to prevention of selective entrapment which would facilitate more uniform dispersion of NPs throughout the ABS matrix. However to ascertain the effect of heat drying on the antibacterial properties of NPs, it is recommended to perform antibacterial tests on the filaments built with preconditioned constituents.

4. RESULTS AND DISCUSSIONS:

4.1. Results and discussion from first phase:

Results obtained from test for 3D printability, mechanical testing, and antibacterial testing of filaments containing 0, 0.5, 1 and 2 wt. % of the filaments have been discussed in this section.

4.1.1 Results from test for 3D printability:

The pure ABS filament and nanocomposite filaments with up to 2 % w/w concentration of MgO NP were successfully printed with the in house 3D printer. The 4% filament could not be printed due to its high diametric error of up to ±0.46 mm. The letters A, U and T were printed with nanocomposite filaments having 0.5 %, 1% and 2% w/w concentrations of MgO respectively whereas the supporting board was printed with pure ABS filament **(fig. 6)**. The 2% filament had success rate of 33.33% for the in-house FDM printer. Since the diametric error for 2% filament was found to be varying from ±.15 mm to ±.22 mm at different places, therefore it might be difficult for the 3D printer gripping gears to grip the filament. In first two iterations, when the 2% filament segment having diameter of 1.75±.22 was fed in the 3D printer, the 3D printer nozzle stopped extruding the filament after some time. In the third iteration, a 2 % filament segment having diameter of 1.75±.15 was fed in the printer and the letter T was successfully printed. This shows that it is possible to print filaments with higher concentration of NP as long as they have a consistent diameter. Letters U and A were observed to have satisfactory build finish whereas the top layer of letter T (built with 2% filament) was observed to be under extruded (Fig. 6).

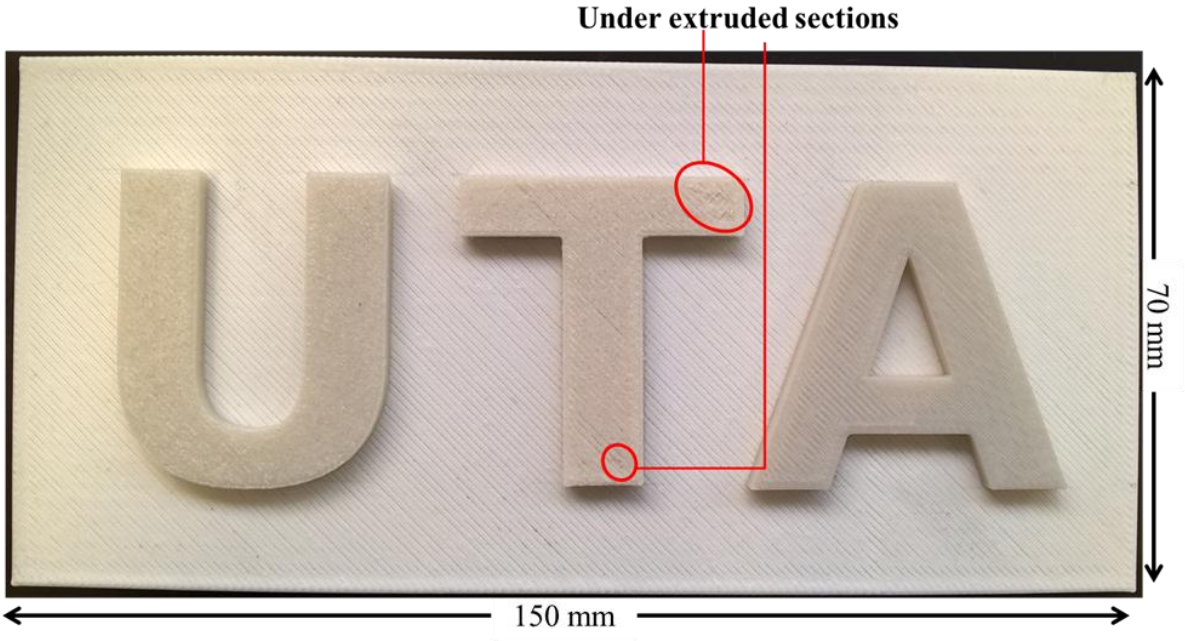

Figure 6: 3D printed sample

Filament type	No. of visible under extruded sections	printing success rate
ABS	0	100%
ABS+MgO (0.5%)	0	100%
ABS+MgO (1%)	0	100%
ABS+MgO (2%)	2	33%
ABS+MgO (4%)	N/A	0%

Table 2: 3D printability of different filaments

4.1.2 Results from tensile testing

The supplied filament and the lab made filaments were compared for their mechanical behaviour under tensile loads. The lab made filament containing no MgO NP (pure ABS) at all was observed to exhibit highest tensile strength of 41.31 Mpa whereas the supplied filament having no MgO (pure ABS) had tensile strength of 39.65 Mpa. The composite filaments exhibited a pattern of decrease in tensile strength and ductility with increasing concentrations of MgO NP in the polymer matrix **(Fig. 7)**. The tensile strengths of filaments containing 0.5 %, 1% and 2 % w/w of MgO were recorded as 36.65 Mpa, 28.17 Mpa and 19 Mpa respectively. It was observed that up to approximately 1% strain, the stiffness of nanocomposite filament containing 0.5 wt. % MgO was greater than that of the supplied ABS

filament. The stiffness of nano composite filaments was greater than the supplied ABS filament only up to strains lower than 1 %. Fig. 7 only compares stress strain curves of the samples that exhibit highest tensile strength in each category. Fig. 8 and 9 show a distribution of Ultimate Tensile Strength and Percent elongation for 4 samples from each filament type. Ductility for lab made filament containing no MgO NP at all was observed to be highest followed by the supplied filament containing no ABS and nanocomposite filaments. It was expected that the nano composite filaments would show a decreasing ductility trend with increasing concentration of MgO NP (Paul et al, 2008) and the results corroborated that ductility decreases with increasing concentration of NP. Almost constant decrement in percent elongation was noticed with increasing concentration of MgO NP in ABS except while going from 0.5 % to 1 %, the percent elongation did not differ considerably.

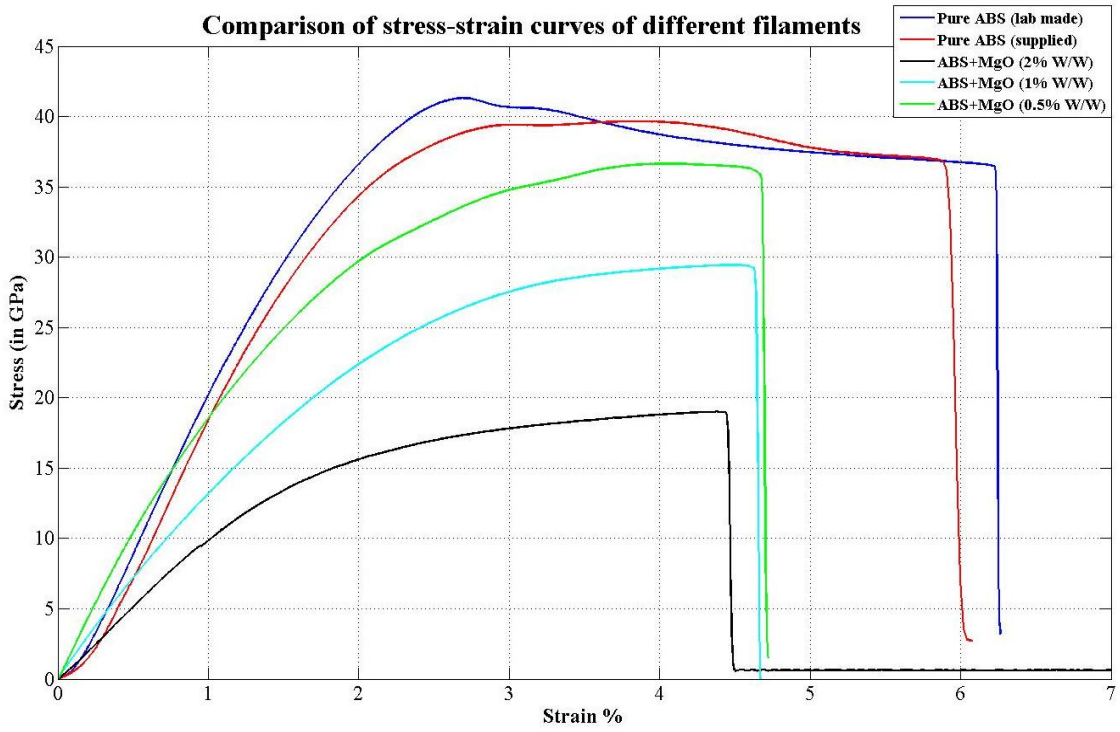

Figure 7: Stress strain curves for different filament types

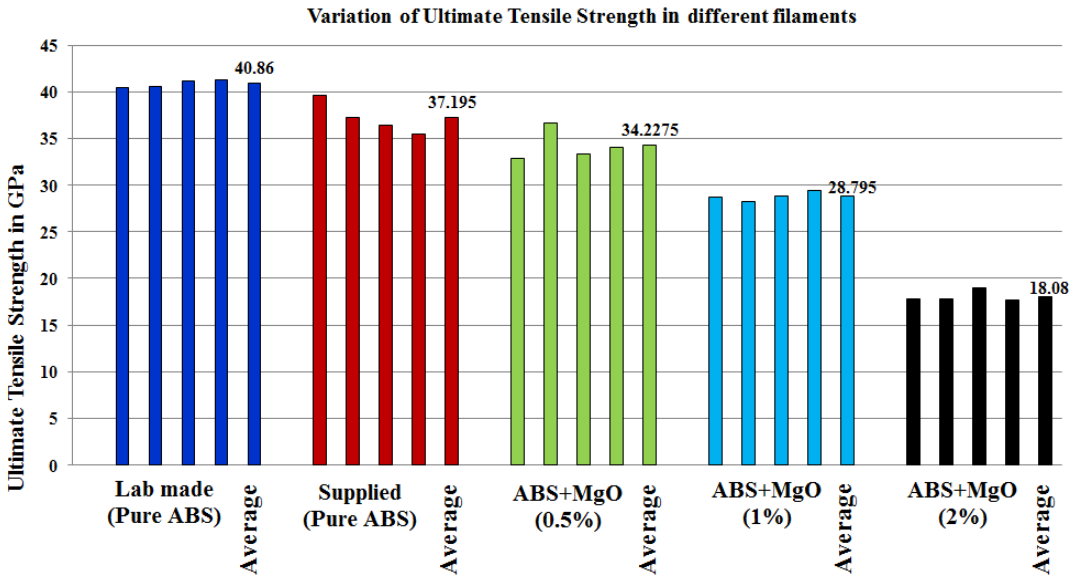

Figure 8: Ultimate Tensile Strength for different filament types

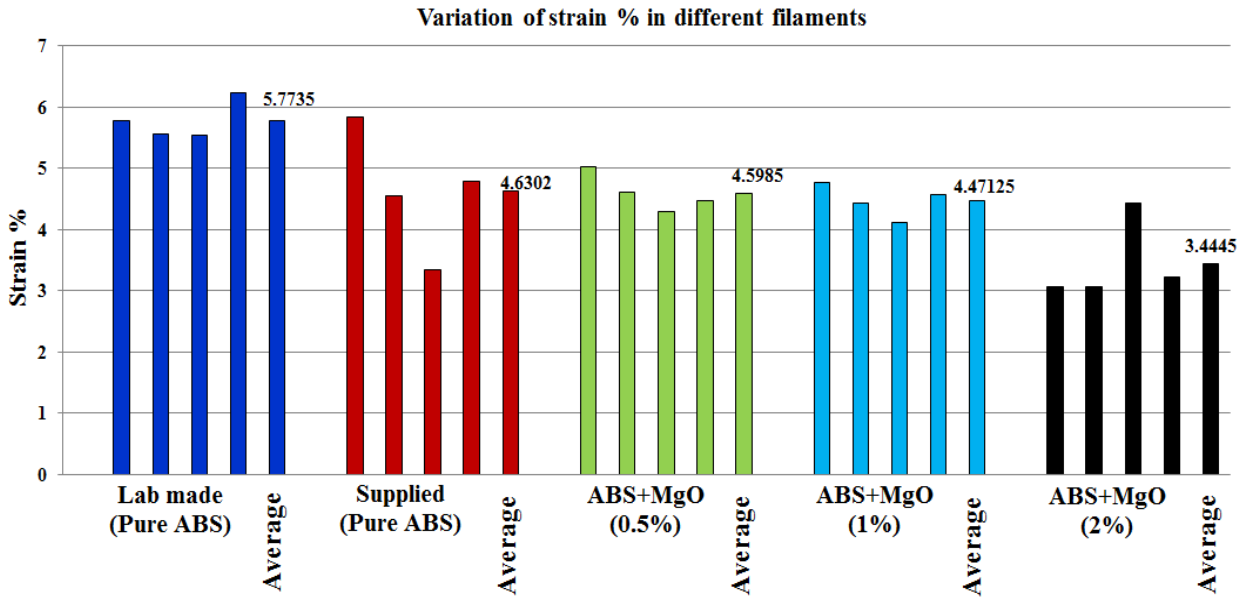

Figure 9: Percent elongation for different filament type

4.1.3 Results from antibacterial testing

The NP showed antibacterial activity against one of the bacteria tested. No growth was observed for *K. pneumoniae*, which suggests that the MgO NP were able to inhibit the growth of this microorganism and therefore present antibacterial properties. For *B. subtilis* and *E. coli*, bacterial growth on the 1% MgO NP NA plates was observed (**Fig.10.**).

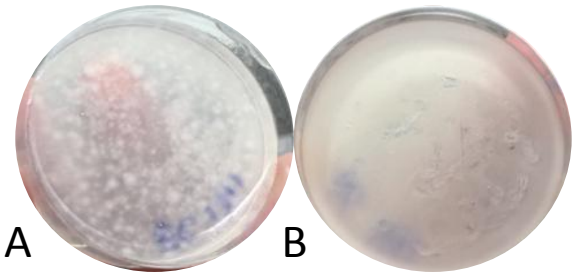

Figure 10: E. coli growth on 1 w.t. % MgO NP NA (A) and NA (B)

The results for the disc diffusion assay are summarized in Table 2. The filaments were found to have antibacterial activity against both gram-positive (*B. subtilis*) and gram-negative bacteria (*K.* pneumoniae and *P. aeruginosa*). The antibacterial properties of NP are dependent on the concentration, with the highest concentration exhibiting the most antibacterial activity. There was inhibition at 0.5 w.t. % MgO for only *B. subtilis*. *K. pneumoniae* and *P. aeruginosa* were both inhibited by filaments containing 1 and 2 w.t. % MgO NP (Figure 10). Of these, the MgO-ABS nanocomposite filament showed maximum sensitivity against *P. aeruginosa* which was listed as critical in WHO's list of multiple drug resistant pathogens.

MgO	**Halo of inhibition (mm) ± SD**				
(w.t. %)	***P. aeruginosa***	***K. pneumoniae***	***A. baumannii***	***E. coli***	***B. subtilis***
0	-	-	-	-	-
0.50	-	-	-	-	4.5 ± 0.7
1	4.5 ± 0.7	4 ± 1.4	-	-	-
2	8.5 ± 0.7	4.33 ± 0.58	-	-	-

Table 3: Disc diffusion assay results for the filaments containing different MgO concentrations, n=2

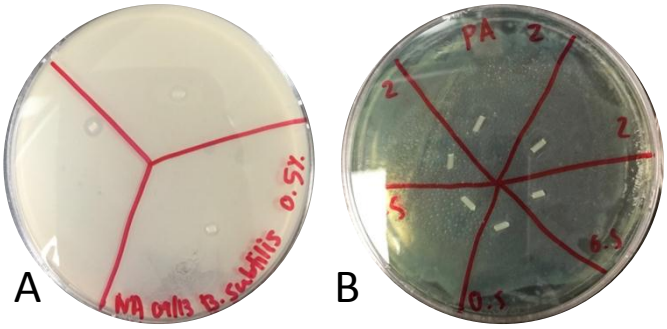

Figure 11: Antibacterial properties of filaments shown for B. subtilis at 0.5 w.t. % (A) and P. aeruginosa at 2 w.t. % (B).

No antibacterial activity for *A. baumannii* and *E. coli* was observed. While there have been previous reports of antibacterial activity of MgO NP against *E. coli*, this has been shown to be dependent on concentration and size of NP. Also, different strains of bacteria are known to exhibit different antimicrobial susceptibilities. A false negative may have been obtained for these microorganisms since there was not a uniform distribution of NP among the surface of the filaments. This affected the overall surface contact with the inoculum and the ability for the NP to demonstrate activity. Nevertheless, antibacterial activity was still shown for other microorganisms.

Furthermore, the repeatability of the results is shown in Fig. 12. Overall, the results obtained suggest that the newly synthesized filaments, doped with MgO NP, have the potential to be used in a wide-range of applications to prevent the growth of certain pathogenic bacteria.

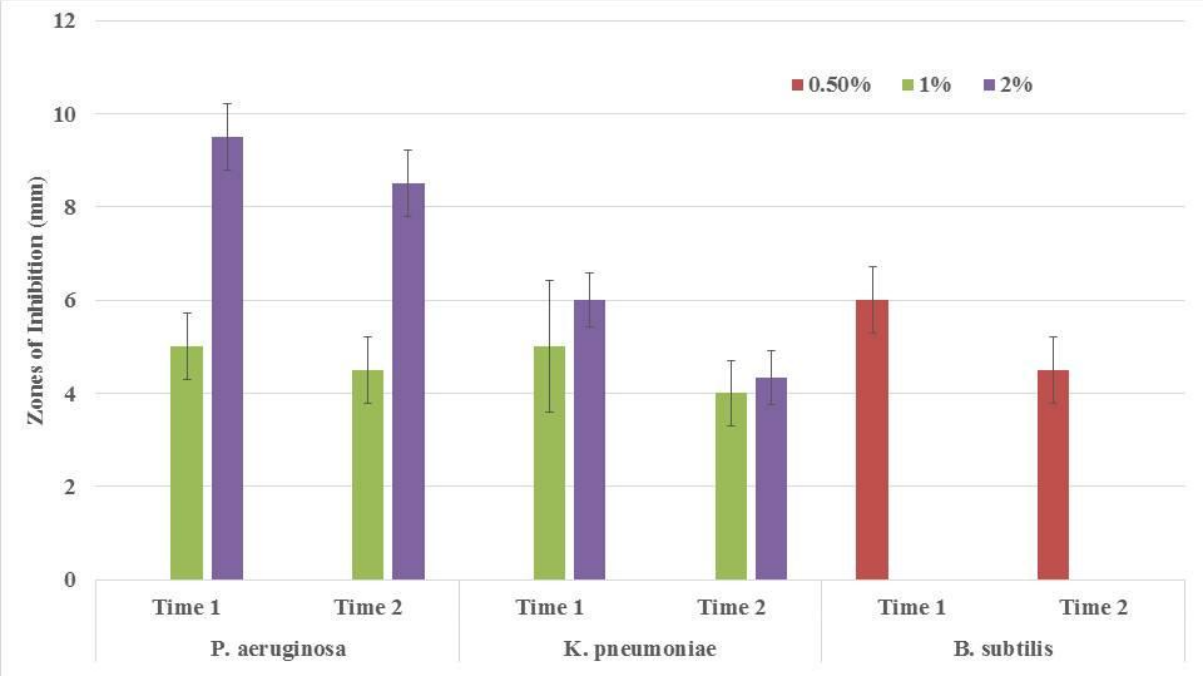

Figure 12: Results for the repeatability of the disc diffusion assay

4.2 Results and discussion from second phase:

Since the filament containing 2 wt. % MgO NPs was found to inhibit microorganisms to the greatest extent as well as 3D printable, results obtained after processing and testing of different types of filament containing only 2 wt.% MgO (Table 1) NPs are discussed in this section.

4.2.1 Effect of pre-conditioning on diametric consistencies of filaments

Fig. 13 shows that all the filaments synthesized from pre-conditioned pellets and NPs had smaller RMSE and thus greater diametric consistency when compared to filament synthesized from unconditioned pellets and NPs (Type 1). The value of RMSE for type 4 filament was the least among other nanocomposite filaments which indicates that diameter becomes more consistent when all of the constituents are pre-conditioned. Moreover it was visible that type 4 filament had lesser number of air bubbles protruding from surface as compared to type 1. Although there was a small decrease in RMSE of diameter while moving from Type 2 to Type 3 filament, it should be noted that only 2 wt. % NPs were present in the mixture. This indicates that heat drying the NPs which only constitute 2% of the mixture would produce diameter similar to when ABS pellets were ground. Moreover the diametric error for type 2 filament was found to be smaller than that of type 3 filament.

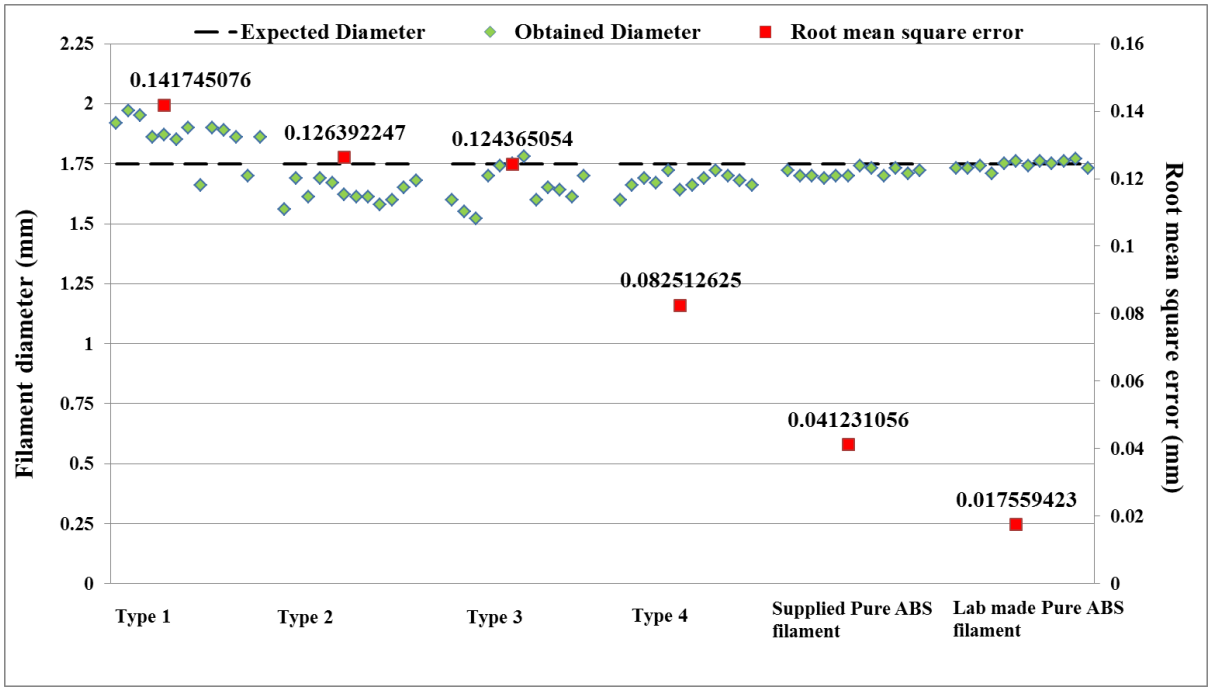

Figure 13: Comparison of diametric consistencies of different filament types listed in Table 1 *(section 3.2.1)*

The results indicate that the presence of volatile impurities in NPs and bigger pellet size adversely affect the diametric consistency of the filament. Heating the NPs contributes to reduction in moisture content in the mixture whereas smaller pellet size is believed to contribute to improved conduction melting and thus reduce the viscosity of ABS inside the barrel (Section 3.1).

4.2.2 Results from void size analysis

Fig. 14 and fig. 15 show the SEM micrograph and void size distribution of samples from different filament types respectively. Type 1 filament was observed to have maximum number of voids sized between 700-800 µm, type 2 and type 3 filament had maximum number of voids sized up to 50 µm whereas type 4 filament had maximum number of voids sized up to 25 µm. It was observed that voids in type 1 filament were closely spaced as compared to those in other filament types. Although the average void size for type 3 filament was less than that of type 2 filament, type 3 filament was observed to have slightly higher number of larger sized voids. The average void size decreased by over 90% as both of the constituents of nanocomposite filament were pre-conditioned as compared to when none was preconditioned (Fig. 16), indicating that processing methods that facilitate removal of volatile impurities from the mixture constituents and from the melt pool (section 4.1) will reduce void size.

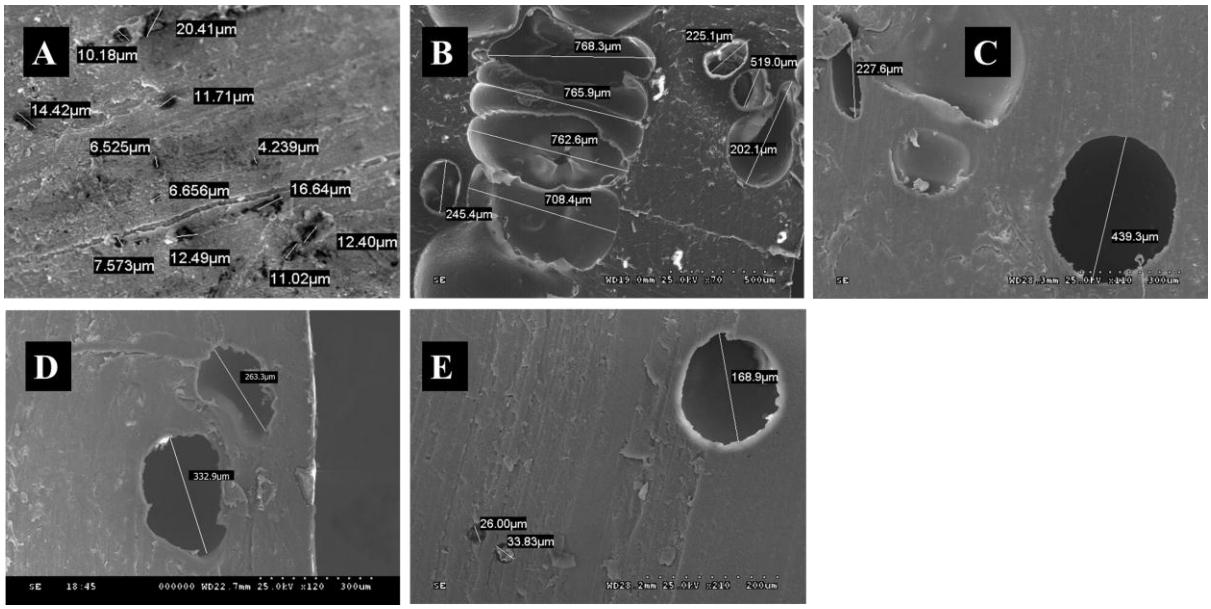

Figure 14: SEM micrograph of voids in supplied (pure ABS filament) (A), Type 1 (B), Type 2 (C), Type 3 (D) and Type 4 (E) filament.

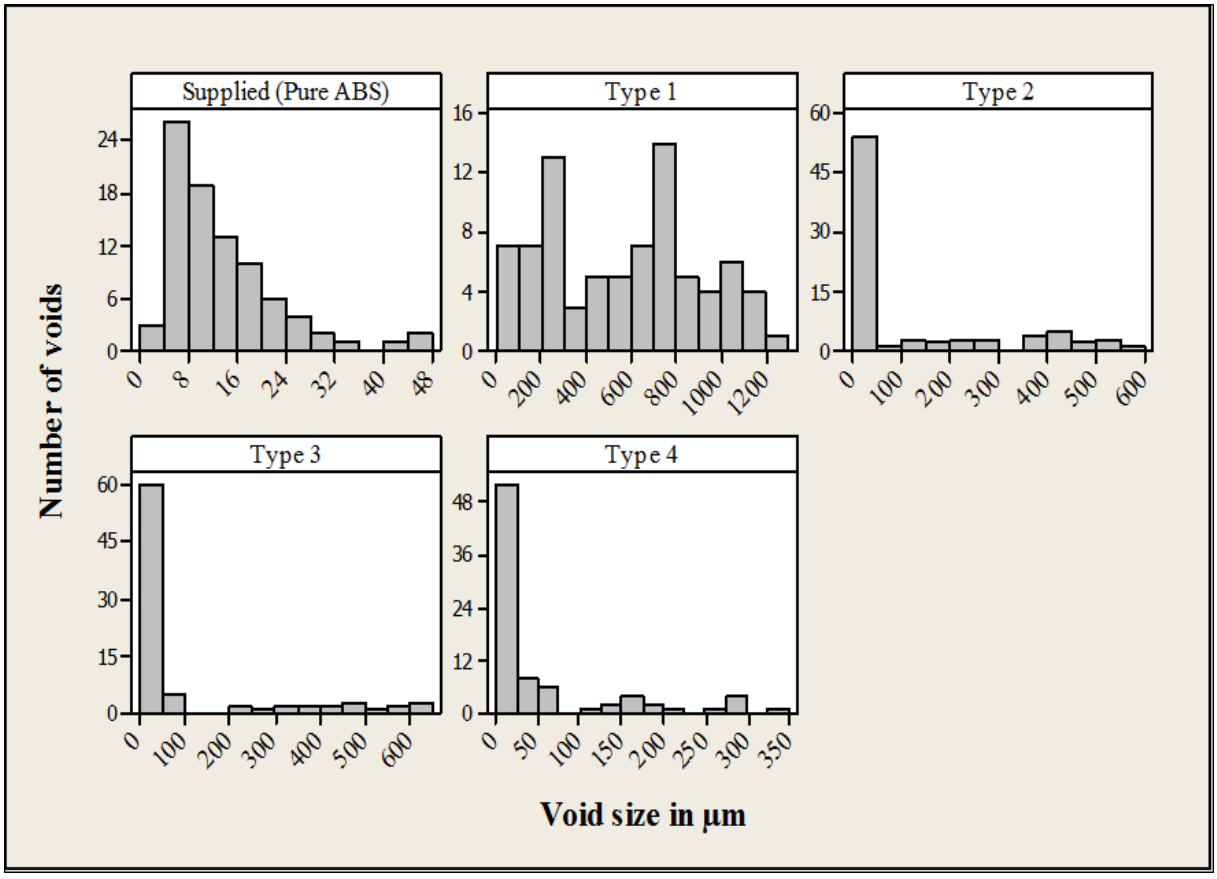

Figure 15: Void size distribution of different filaments

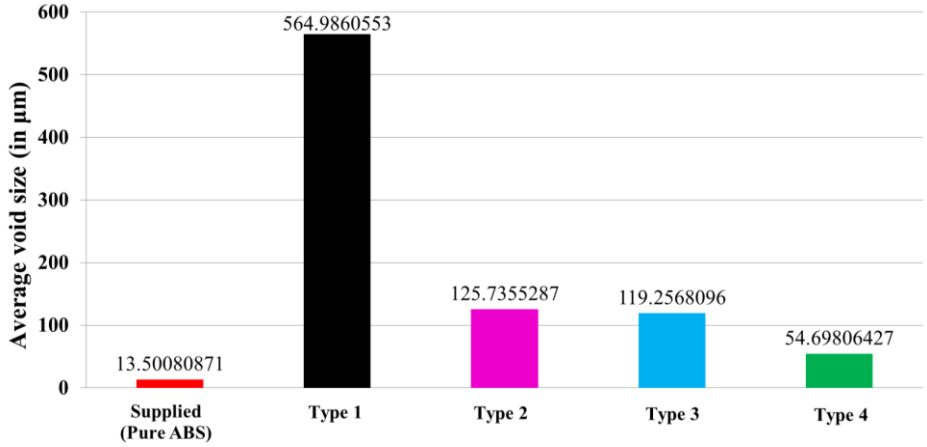

Figure 16: Average void size for different filaments

4.2.3 Results from mechanical testing

Fig. 17 shows the stress-strain curves of different types of filament and only compares filament samples having maximum strength in their respective category. Pure ABS filaments were observed to exhibit maximum UTS and ductility as expected. Among the nanocomposite ABS-MgO filaments, Type 4 filament was observed to have maximum UTS while Type 1 was observed to have minimum. Stiffness of the filaments was observed to be increasing to a greater extent when the NPs were heat-dried in comparison to when the pellets were ground. Stiffness for type 4 filament was recorded as highest among other nanocomposites and was even higher than the supplied pure ABS filament up to approximately 1.25 % strain. Results indicate that pre-conditioning the constituents increases the tensile strength and stiffness of the filament at lower strain values, and presence of volatile impurities adversely affects these mechanical properties of the filament.

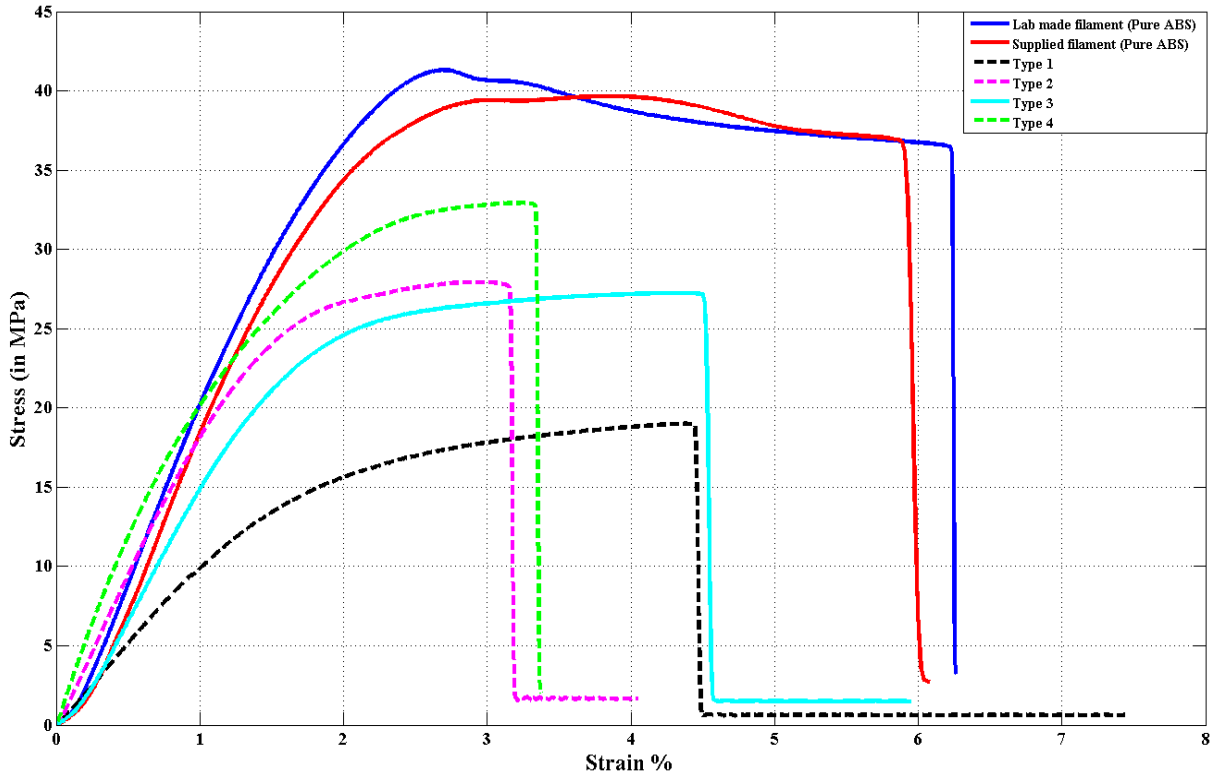

Figure 17: Stress-strain curves for different filament types

Fig. 18 and fig. 19 compare the average tensile strength and average percent elongation at break for each filament type. The average value of tensile strength was observed to be highest for type 4 filament, whereas type 2 filament had more tensile strength than that of type 3 filament. Although NPs constitute only 2 % of the mixture, heating of NPs improved the tensile strength to a greater extent as compared to grinding the ABS pellets. Slightly higher number of bigger voids in type 3 filament was believed to be the reason for its lower UTS than that of Type 2 filament. Moreover it was observed that by pre-conditioning the mixture constituents, tensile strength of the filament increased by more than 84 %. The tensile strength of type 1 (unconditioned) filament was only 49 % of that of supplied pure ABS filament, whereas the tensile strength of the type 4 multifunctional filament (made from pre-conditioned NPs and pellets) was found to be approximately 90% of the supplied pure ABS filament.

The ductility of type 3 filament was greater than all other types of multifunctional filament. It was interesting to observe that every time the NPs were heated, the fracture strain decreased by a small value (as the fracture strain percent of type 1 filament was greater than that of type 2 whereas fracture strain percent of type 3 filament was greater than that of type 4).

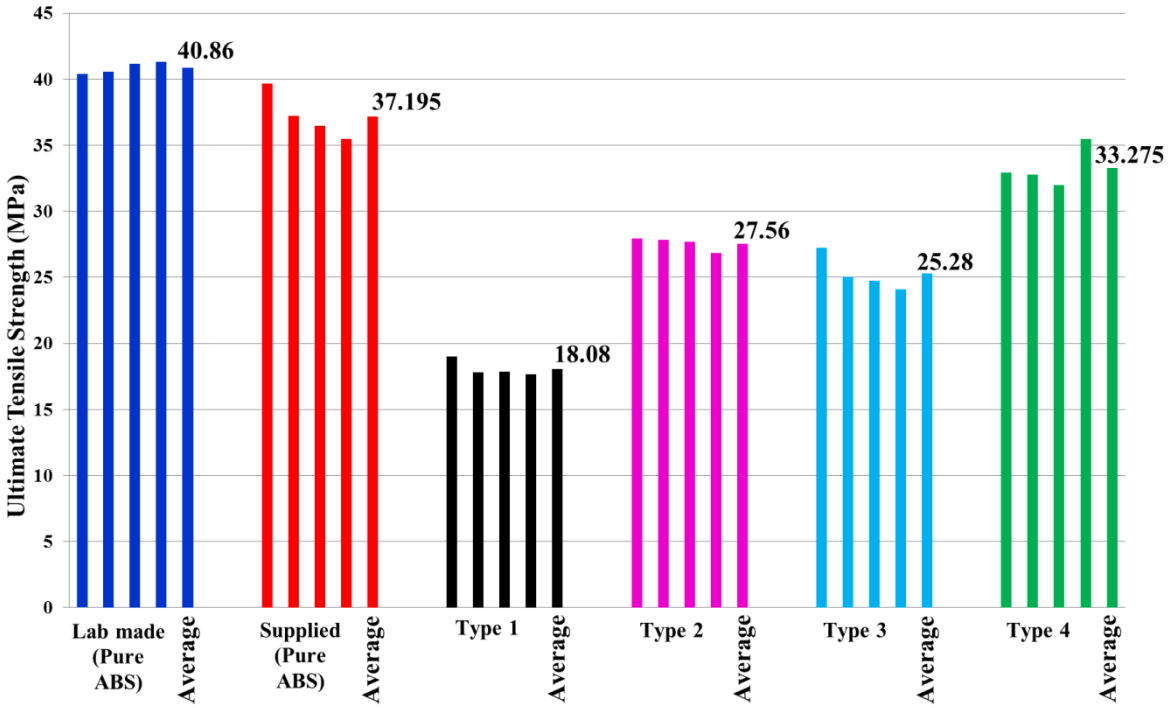

Figure 18: Ultimate Tensile Strength for different filament types

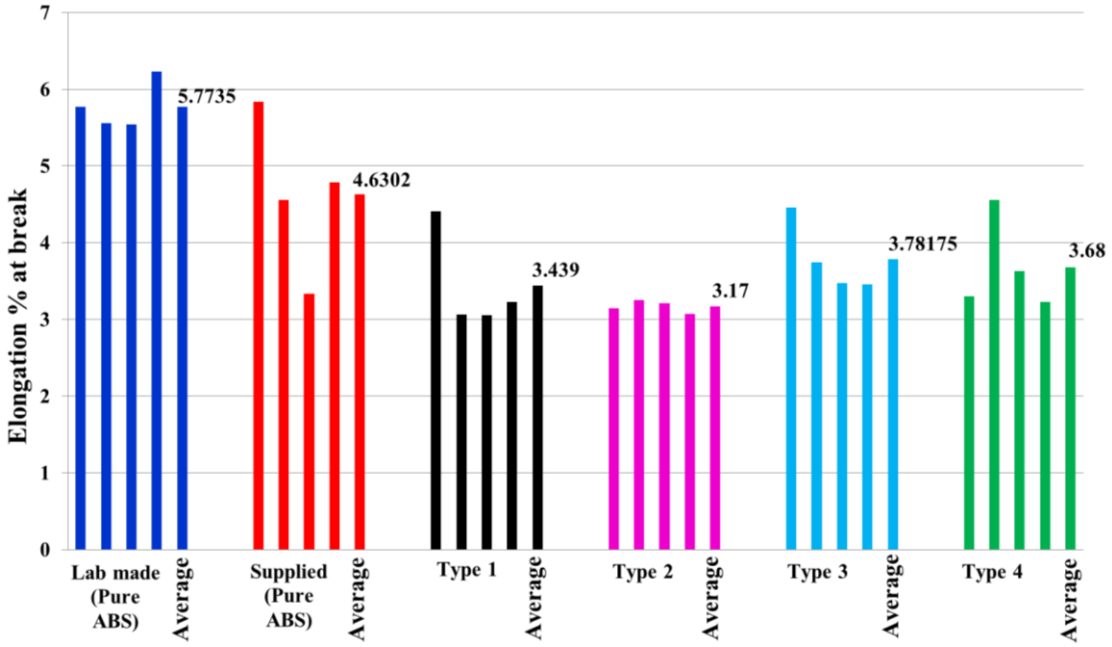

Figure 19: Elongation percent at break for different filament types

Although voids in the order of microns are considered to toughen the rubber toughened polymers (Michler et al., 2013), large average void size and closely spaced voids were believed to be causing premature failure in type 1 filament; presence of voids and heterogeneity can also induce thermal stresses inside the nano composite multifunctional

filament resulting in premature failure (Awaja et al., 2016). Moreover the type 1 filament was observed to have lesser crazing growth before fracture unlike pure ABS or type 4 filament. Ayewah et al. (2010) noticed a similar phenomenon with polystyrene (PS)-single wall carbon nanotube (SWCNT) composite. With increase in concentration of SWCNT in PS, the capability of sustaining a craze growth was observed to be deteriorating in the composite material. As the voids coalesce, crazing follows (Kinloch, Young), (Desai et al., 2011), (Focatiis et al., 2008) and ultimately crack propagates, but if the void size is too large and voids are closely spaced, coalescence of voids is believed to pre-dominate the growth of crazing. Due to the presence of voids of larger average size within type 1 filament, it was believed that voids coalesced before crazing thus making the filament brittle whereas for filaments built with preconditioned constituents, since the average void size reduced by up to 90.31 % therefore crazing growth could be sustained for a comparatively longer time thus increasing the fracture strain and UTS.

4.2.4 Results from test for 3D-printability

Since the filament of type 4 exhibited greatest diametric consistency and tensile strength therefore type 4 filament was tested for 3D printability using in house FDM printer. The letter T was successfully 3D printed with this filament in single iteration and the build was found to have a small under extruded section.

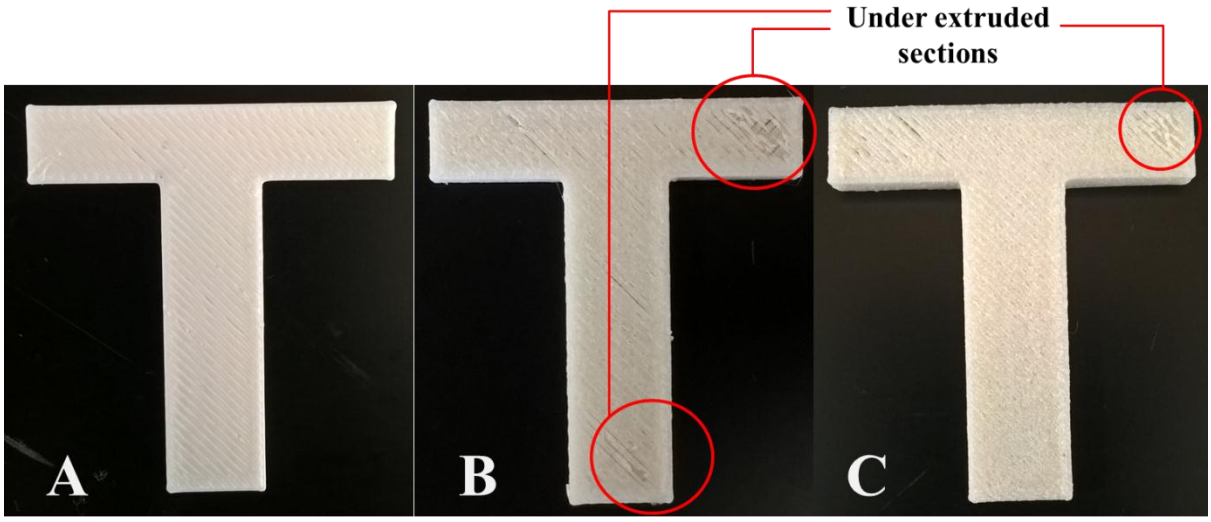

Figure 20: Alphabets printed with supplied pure ABS (A), type 1 filament (B) and type 4 filament (C)

Fig. 20 shows different objects printed with different filaments. The object printed with type 1 filament had at least 2 visible under extruded sections whereas the one printed

with type 4 filament had one such section. Problems such as layer misalignment were commonly observed in all 3 objects and these are believed to be the 3D printer issue rather than the filament issue. The improved diametric consistency obtained as a result of grinding the pellets and heating the NPs is believed to be the reason for improved 3D printability. The test results indicate that processing methods that facilitate removal of volatile impurities from the mixture and from the melt, improve 3D printability of the filament. Fig. 21 shows the completed object printed with supplied pure ABS filament and filaments containing 0.5, 1, 2 w/w % MgO in ABS. Alphabets U, T and A were printed with 0.5 wt. %, type 4 and 1 wt. % filaments respectively whereas the supporting board was printed with pure ABS filament.

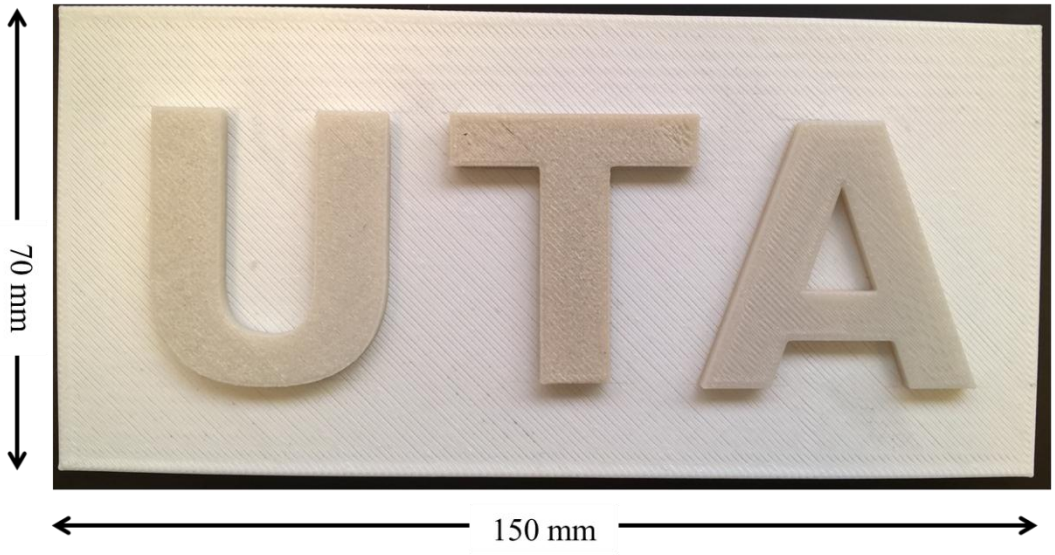

Figure 21: Object printed with the nanocomposite and pure ABS filaments

5. CONCLUSION

5.1. With the two-step process of extrusion of NP-polymer blend followed by 3D printing, it is possible to make plastic objects around us resistant to pathogens known to have developed antibiotic resistance against several drugs in a cost effective manner. The 1% and 2% nanocomposite filament samples were observed to inhibit *Pseudomonas aeruginosa* to the greatest extent, followed by *Klebsiella pneumoniae*, however the 0.5% filament could only inhibit *Bacillus subtilis*. This method can also be used to introduce other NP such as copper, silver, etc. that are known to be effective against wide range of bacteria (Plaza, 2015). Apart from antibacterial property, several other functionalities depending on the properties of NP can be added in the 3D printer inks using this method.

Antibacterial activities were observed to increase with increasing concentrations of NP, however poor 3D printability and relatively lower strength were also observed with increasing concentrations. It was observed that concentration of NP affects diametric consistency; moreover voids and bubbles were noticeable with unaided eyes in filament containing 4 wt. % of MgO NP but were not observed in pure ABS filament suggesting that increasing concentration of NP causes formation of noticeable bubbles and voids which in turn adversely affects the diametric consistency. Considering the presence of voids in nanocomposite filament, mechanical failure might be driven by void coalescence; improving the filament strength in that case would require reduction of void size. After first phase of study it was believed that reduction in void size would not only improve mechanical properties but can also improve 3D printability of the filament as the formation of voids and bubbles on filament surface causes diameter to go inconsistent. Improving the 3D printability and strength of filament with higher concentration of NP (more than 2 wt. % in this case) can be a step forward in using extrusion and additive manufacturing for building smart composite structures.

5.2. In the second phase it was observed that the deteriorating mechanical properties and 3D printability of the filaments with increasing NP concentration were greatly improved with pre-conditioning of the mixture constituents. Results show that presence of volatile impurities (moisture) not only affects the mechanical properties but also the diametric consistency of the ABS-MgO filament and that reducing pellet size and heat-drying the NPs reduce the adverse effect of moisture on mechanical properties and diametric consistency.

Results from void size analysis and mechanical tests show that irregularities (voids) produced due to moisture were the reason behind deteriorating UTS of the ABS-MgO filament. When the mixture was made from ground pellets and heat dried NPs, the average void size inside the extruded filament reduced by more than 90 % and UTS of the extruded filament increased by over 84%.

When the hygroscopic NPs were heat dried and then mixed with ground ABS pellets, the RMSE from the expected value of 1.75 mm, reduced by approximately 42% indicating large improvements in diametric consistency due to removal of bubbles which are formed as a result of presence of volatile impurities in mixture constituents and the melt. Increased diametric consistency improved the 3D printability of the filament and a test object was

successfully printed with type 4 filament in the first iteration whereas the type 1 filament took 3 iterations for printing the same object.

Since type 4 filament contains same concentration of MgO NPs as type 1, therefore same extent of antibacterial activity can be expected at an improved 3D printability and at a tensile strength which is over 184 % of that of type 1 and very close (about 90 %) to that of the pure ABS filament.

6. REFERENCES:

1. ICSC 0504 – Magnesium Oxide (2010) retrieved from http://www.ilo.org/dyn/icsc/showcard.display?p_card_id=0504.

2. Dunlop and Fratzl Bioinspired composites: Making a tooth mimic (2015).

3. Guo X., Gao H. (2006) Bio-Inspired Material Design and Optimization. In: Bendsøe M.P., Olhoff N., Sigmund O. (eds) IUTAM Symposium on Topological Design Optimization of Structures, Machines and Materials. Solid Mechanics and Its Applications, vol 137. Springer, Dordrecht.

4. Wegst, U.G., Bai, H., Saiz, E., Tomsia, A.P., Ritchie, R.O., 2015. Bioinspired structural materials. Nature Materials 14, 23 – 36. doi:10.1038/nmat4089

5. Yoseph Bar-Cohen, Biomimetics: biologically Inspired Technologies, CRC Press, 2005 (310).

6. Integrated Design of Multiscale, Multifunctional Materials and Products By David L. McDowell, Jitesh H. Panchal, Hae-Jin Choi, Carolyn Conner Seepersad, Janet K. Allen and Farrokh Mistree ISBN: 978-1-85617-662-0.

7. Suva, L. J. and Griffin, R. J. (2012), The irradiation of bone: Old idea, new insight. J Bone Miner Res, 27: 747–748. doi:10.1002/jbmr.1586

8. Zhu, H.; Zhu, S.; Jia, Z.; Parvinian, S.; Li, Y.; Vaaland, O.; Hu, L.; Li, T. Anomalous scaling law of strength and toughness of cellulose nanopaper. Proc. Natl. Acad. Sci. U. S. A. 2015, 112 (29), 8971−8976 doi: 10.1073/pnas.1502870112.

9. Hirsch EB, Raux BR, Lancaster JW, Mann RL, Leonard SN (2014) Surface Microbiology of the iPad Tablet Computer and the Potential to Serve as a Fomite in Both Inpatient Practice Settings as Well as Outside of the Hospital Environment. PLoS ONE 9(10): e111250. https://doi.org/10.1371/journal.pone.0111250.

10. Dunn, R. R., Fierer, N., Henley, J. B., Leff, J. W., & Menninger, H. L. (2013). Home Life: Factors Structuring the Bacterial Diversity Found within and between Homes. PLoS ONE, 8(5), e64133. http://doi.org/10.1371/journal.pone.0064133.

11. Peleg, A. Y., & Hooper, D. C. (2010). Hospital-Acquired Infections Due to Gram-Negative Bacteria. The New England Journal of Medicine, 362(19), 1804–1813. http://doi.org/10.1056/NEJMra0904124

12. Poza M, Gayoso C, Go´mez MJ, Rumbo-Feal S, Toma´s M, et al. (2012) Exploring Bacterial Diversity in Hospital Environments by GS-FLX Titanium Pyrosequencing. PLoS ONE 7(8): e44105. doi:10.1371/journal.pone.0044105.

13. Bacterial Colonization of Toys in Neonatal Intensive Care Cots Mark W. Davies, Samuel Mehr, Suzanne T. Garland, FANZCOG‡; and Colin J. Morley Pediatrics Aug 2000, 106 (2) e18;

14. Buttery JP, Alabaster SJ, Heine RG, et al. Multiresistant Pseudomonas aeruginosa outbreak in a pediatric oncology ward related to bath toys. Pediatr Infect Dis J. 1998;17:509–513

15. Antibiotic efficacy and microbial virulence during space flight (David M. Klaus and Heather N. Howard, 2006). http://dx.doi.org/10.1016/j.tibtech.2006.01.008.

16. Otter, J.A. and French, G.L. (2009), Bacterial contamination on touch surfaces in the public transport system and in public areas of a hospital in London. Letters in Applied Microbiology, 49: 803–805. doi:10.1111/j.1472-765X.2009.02728.x.

17. Dye, C. (2014). After 2015: infectious diseases in a new era of health and development. Philosophical Transactions of the Royal Society B: Biological Sciences, 369(1645), 20130426. http://doi.org/10.1098/rstb.2013.0426.

18. Ventola, C. L. (2015). The Antibiotic Resistance Crisis: Part 1: Causes and Threats. Pharmacy and Therapeutics, 40(4), 277–283.

19. Garbati MA, Al Godhair AI. The growing resistance of Klebsiella pneumoniae; the need to expand our antibiogram: case report and review of the literature. Afr J Infect Dis. 2013;7:8–10.

20. Cabot G, Zamorano L, Moyà B, Juan C, Navas A, Blázquez J, Oliver A. 2016. Evolution of Pseudomonas aeruginosa antimicrobial resistance and fitness under low and high mutation rates. Antimicrob Agents Chemother60:1767–1778. 10.1128/AAC.02676-15

21. World Health Organization. 2013. Mortality and global health estimates. Geneva, Switzerland: World Health Organization.

22. M. Coultier, D. Mantovani, F. Rosei Special focus on materials Review. Antibacterial coatings: challenges, perspectives, and opportunities. Trends Biotechnol., 33 (2015), pp. 637–652.

23. The Agency for Science, Technology and Research (A*STAR). (2015, May 14). Highly conducive material for 3D-printing of circuits. ScienceDaily. Retrieved April 14, 2017 from www.sciencedaily.com/releases/2015/05/150514132732.htm.

24. Mahfuz, H., Hasan, M. M., Rangari, V. K. and Jeelani, S. (2007), Reinforcement of Nylon-6 Filaments with SiO2 Nanoparticles and Comparison of Young's Modulus with Theoretical Bounds. Macromol. Mater. Eng., 292: 437–444. doi:10.1002/mame.200600417.

25. R.Y. Pelgrift, A.J. Friedman Nanotechnology as a therapeutic tool to combat microbial resistance Adv. Drug Deliv. Rev., 65 (2013), pp. 1803–1815 http://dx.doi.org/10.1016/j.addr.2013.07.011

26. Tillotson, G. S., & Theriault, N. (2013). New and alternative approaches to tackling antibiotic resistance. F1000Prime Reports, 5, 51. http://doi.org/10.12703/P5-51.

27. L. Zhang, D. Pornpattananangkul, C.-M. J. Hu, and C.-M. Huang, "Development of nanoparticles for antimicrobial drug delivery," Current Medicinal Chemistry, vol. 17, no. 6, pp. 585–594, 2010. DOI: 10.2174/092986710790416290. Source: PubMed.

28. Nurit Beyth, Yael Houri-Haddad, Avi Domb, Wahid Khan, and Ronen Hazan, "Alternative Antimicrobial Approach: Nano-Antimicrobial Materials," Evidence-Based Complementary and Alternative Medicine, vol. 2015, Article ID 246012, 16 pages, 2015. doi:10.1155/2015/246012.

29. Gokulakrishnan et al., 2012 R. Gokulakrishnan, S. Ravikumar, J.A. Raj. In vitro antibacterial potential of metal oxide nanoparticles against antibiotic resistant bacterial pathogens Asian Pac. J. Trop. Dis., 2 (5) (2012), pp. 411–413. http://dx.doi.org/10.1016/S2222-1808(12)60089-9.

30. Huang, L., Li, D., Lin, Y. et al. Chin.Sci.Bull. (2005) 50: 514 doi:10.1007/BF02897474.

31. Jin, T. & He, Y. J Nanopart Res (2011) 13: 6877. doi:10.1007/s11051-011-0595-5

32. Slama, T. G. (2008). Gram-negative antibiotic resistance: there is a price to pay. Critical Care, 12(Suppl 4), S4. http://doi.org/10.1186/cc6820.

33. John R. Wagner Jr. Eldridge M. Mount III Harold F. Giles Jr. EXTRUSION: the definitive processing guide and handbook Second Edition ISBN: 978-1-4377-3481-2. (p. 9, 49, 53, 401, 603).

34. Effect of Fiber Content on the Aspect Ratio of Process-Induced Microvoids and the Implications to the Tensile Properties of Composite Laminates J. P. ANDERSON and M. C. ALTAN Conference Paper September 2014 DOI: 10.13140/2.1.4211.1369 Conference: American Society for Composites 29th Technical Conference, At La Jolla, CA USA.

35. Mudradi Sudheer, Ravikantha Prabhu, Kandavalli Raju, and Thirumaleshwara Bhat, "Effect of Filler Content on the Performance of Epoxy/PTW Composites," Advances in Materials Science and Engineering, vol. 2014, Article ID 970468, 11 pages, 2014. doi:10.1155/2014/970468.

36. Hwang, S., Reyes, E.I., Moon, K. et al. Journal of Elec Materi (2015) 44: 771. doi:10.1007/s11664-014-3425-6

37. Tang, Zhen-Xing, & Lv, Bin-Feng. (2014). MgO nanoparticles as antibacterial agent: preparation and activity. Brazilian Journal of Chemical Engineering, 31(3), 591-601. https://dx.doi.org/10.1590/0104-6632.20140313s00002813

38. Stauber, C.E.; Walters, A.; de Aceituno, A.M.F.; Sobsey, M.D. Bacterial Contamination on Household Toys and Association with Water, Sanitation and Hygiene Conditions in Honduras. Int. J. Environ. Res. Public Health 2013, 10, 1586-1597.

39. Martínez-Bastidas, T., Castro-del Campo, N., Mena, K. D., Castro-del Campo, N., León-Félix, J., Gerba, C. P., & Chaidez, C. (2014). Detection of pathogenic micro-organisms on children's hands and toys during play. Journal of Applied Microbiology, 116(6), 1668-1675. DOI: 10.1111/jam.12473

40. Bauer, A. W., Kirby, W. M. M., Sherris, J. C., & Turck, M. (1966). Antibiotic susceptibility testing by a standardized single disk method. American journal of clinical pathology, 45(4), 493

41. Extrusion of Polymers Theory & Practice (2nd Edition) Chan I Chung, 2011 (Page 29).

42. Vera-Sorroche J, Kelly A, Brown E, Coates P, Karnachi N, Harkin-Jones E, Li K, Deng J (2013) Thermal optimisation of polymer extrusion using in-process monitoring techniques. Appl Therm Eng 53(2):405–413. doi:10.1016/j.applthermaleng.2012.04.013

43. Gupta, S.S., Solanki, N. & Serajuddin, A.T.M. AAPS PharmSciTech (2016) 17: 148. doi:10.1208/s12249-015-0426-6

44. Hamouda, T.; Baker, J.R. (2000). "Antimicrobial mechanism of action of surfactant lipid preparations in enteric Gram-negative bacilli." Journal of Applied Microbiology 89(3). http://hdl.handle.net/2027.42/98818.

45. Sawai, J., Kojima, H., Igarashi, H. et al. World Journal of Microbiology and Biotechnology (2000) 16: 187. doi:10.1023/A:1008916209784

46. Yamamoto, O., Sawai, J. and Sasamoto, T., Change in antibacterial characteristics with doping amount of ZnO in MgO-ZnO solid solution. International Journal of Inorganic Materials, 2, 451-454 (2000)

47. Lin, YJ., Xu, XY., Huang, L. et al. J Mater Sci: Mater Med (2009) 20: 591. doi:10.1007/s10856-008-3585-0

48. Yamamoto, O., Ohira, T., Alvarez, K. and Fukuda, M., Antibacterial characteristics of CaCO3-MgO composites. Materials Science and Engineering B, 173, 208-212 (2010).

49. Yamamoto, O., Fukuda, T., Kimata, M., Sawai, J. and Sasamoto, T., Antibacterial characteristics of MgO-mounted spherical carbons prepared by carbonization of ion-exchanged resin. Journal of the Ceramic Society of Japan, 109, 363-365 (2001)

50. Sawai, J., Kojima, H., Igarashi, H., Hasimoto, A., Shoji, S., Takehara, A., Sawaki, T., Kokugan, T. and Shimizu, M., Escherichia coli damage by ceramic powder slurries. Journal of Chemical Engineering of Japan, 30, 1034-1039 (1997)

51. D. Paul, L. Robeson Polymer nanotechnology: nanocomposites. Polymer, 49 (2008), pp. 3187–3204. http://dx.doi.org/10.1016/j.polymer.2008.04.017

52. G.H. Michler, H.-H.K.-B. von Schmeling The physics and micro-mechanics of nano-voids and nano-particles in polymer combinations Polymer, 54 (2013), pp. 3131–3144 http://dx.doi.org/10.1016/j.polymer.2013.03.035

53. F. Awaja, S. Zhang, M. Tripathi, A. Nikiforov, N. Pugno Cracks, microcracks and fracture in polymer structures: formation, detection, autonomic repair Prog Mater. Sci, 83 (2016), pp. 536–573 http://dx.doi.org/10.1016/j.pmatsci.2016.07.007

54. G.H. Michler, H.-H.K.-B. von Schmeling The physics and micro-mechanics of nano-voids and nano-particles in polymer combinations Polymer, 54 (2013), pp. 3131–3144 http://dx.doi.org/10.1016/j.polymer.2013.03.035

55. F. Awaja, S. Zhang, M. Tripathi, A. Nikiforov, N. Pugno Cracks, microcracks and fracture in polymer structures: formation, detection, autonomic repair Prog Mater. Sci, 83 (2016), pp. 536–573 http://dx.doi.org/10.1016/j.pmatsci.2016.07.007.

56. D.O.O. Ayewah, D.C. Davis, R. Krishnamoorti, D.C. Lagoudas, H.-J. Sue, M. Willson A surfactant dispersed SWCNT-polystyrene composite characterized for electrical and mechanical properties Compos A Appl Sci Manuf, 41 (2010), pp. 842–849

57. A.J. Kinloch and R.J. Young, "Fracture behaviour of polymers" DOI 10.1007/978-94-017–1594–2,p.69-70,1995

58. Desai C.K., Kumar A.S., Basu S., Parameswaran V. (2011) Measurement of Cohesive Parameters of Crazes in Polystyrene Films. In: Proulx T. (eds) Experimental and Applied Mechanics, Volume 6. Conference Proceedings of the Society for Experimental Mechanics Series. Springer, New York, NY

59. D.S.A. De Focatiis, C.P. Buckley Determination of craze initiation stress in very small polymer specimens Polym. Test., 27 (2008), p. 136-145 http://dx.doi.org/10.1016/j.polymertesting.2007.08.006

60. Palza, H. Antimicrobial Polymers with Metal Nanoparticles. Int. J. Mol. Sci. 2015, 16, 2099-2116.

61. Polymer Extrusion Cooling for the 21st Century. A white paper by: Wesley J. Sipe, Mechanical Systems Manager, GAI Consultants on behalf of: NOVATEC, Inc. Baltimore, MD USA, 2012.

7. APPENDIX

The extruder requires mechanical and electrical modifications so as to obtain specific set of results. A hopper, hopper cover, spacer for the winder unit and a tripod stand for the winder shaft were designed and then 3D printed using FDM printer. A larger hopper would allow in feeding of polymer-NP mixture in larger quantity, a hopper cover would prevent dust particles from entering the extruder barrel, a spacer was designed and fabricated to prevent axial movement of the filament spool on shaft and thus prevent it from stopping frequently and an easy to remove tripod stand was designed and fabricated to support the winder shaft. In order to extrude ABS, correct current and voltage should be set up in the extruder. The manufacturer recommended current for smooth running of extruder is 1.4-1.6 amp, adequate current assists in melting the polymer initially and in continuous rotation of auger at the later stages (at later stages power is dissipated against resistive forces developed by highly viscous polymers) (Chung, 2011, 27). Current in the unit was adjusted using set screws to lie in the range 1.4-1.6 amp and the voltage to 12 Volts (manufacturer recommended). Diametric consistency of the filament is important to achieve good 3D printability in a filament and the build finish as the FDM printer extruder gears might find it difficult to grip a diametric inconsistent filament. In order to achieve diametrical consistencies in the extruded filament, development of an effective cooling mechanism for the hot extruded filament was very important. Extrudate must be cooled rapidly below its glass transition temperature so that desired size and shape could be attained. Usually water cooled systems are considered to be more effective for extracting large amount of heat from hot filament in short time (Sipe, 2012) however they can also produce thermal stresses in the filament; furthermore, water cooling apparatus requires a pulling mechanism to draw the hot filament out of the extruder nozzle, is expensive to set and requires more space. Although water cooling was complex to set up in the bench-top extruder unit, the feasibility of water cooling mechanism was checked. Samples from other cooling mechanisms such as air cooling were also obtained and then all the filament samples were inspected for diametric consistency. All the samples were obtained by extruding pure ABS pellets at manufacturer recommended temperature of 185 °C. It was observed that the filament obtained by water cooling was not straight due to absence of configured pulling mechanisms in the unit. Air cooling was therefore implemented in the final setup. The air fan that came with the extruder (rated at 12 V & .16 A) was replaced with a more powerful Thermaltake CPU fan (rated at 12 V & .20 A). New fan has a maximum air flow capacity of 23.1 CFM compared to 18 CFM of

the custom fan. Due to larger air flow, the nozzle gets cooled rapidly along with the extrudate. As the nozzle gets cooled, the PID unit connected to the extruder displays rapidly falling temperature on the nozzle and motor stops due to resistance from highly viscos ABS inside the barrel. To counter this problem, it was ensured that the fiberglass insulation covers the extruder nozzle along with the thermocouple that sits in the hole on nozzle. Next, a suitable height for mounting the extruder was determined by measuring filament diameters at different heights. It was observed that at greater heights, larger amount of filament hangs beneath the nozzle and consequently exerts larger pulling force (due to larger hanging weight) on the still hot filament, this causes thinning of filament; on the other hand at smaller heights above ground, the filament extruded was observed to have twists and kinks. An optimized mounting height of 3 ft. was chosen after checking diameter consistency and straightness of extruded filament at different heights. The filament obtained after finalising the setup and mounting had a diameter of 1.75±.04 mm and was tested for 3D printability. The pure ABS filament obtained was successfully 3D printed.

Although pure ABS could be extruded at a temperature of 185 °C, the extruder motor was observed to be stopping abruptly after few minutes of extrusion of ABS-MgO NP mixture at this temperature. The reason for this abrupt stopping of extruder was believed to be clogging of filament extruder nozzle by NP. Processing temperature was therefore increased to reduce viscosity of molten pool inside the barrel which in turn would facilitate flow of the mixture. The processing temperatures were determined by performing several iterations and then choosing a temperature at which the motor could run uninterruptedly. Even after the extruder nozzle reached the set temperature, the extruder motor was not switched ON until at least 20 minutes. This allowed pre-melting of ABS inside the barrel and thus prevents the motor from stopping while the auger is contributing to generate shear heat. The extruder nozzle was placed at a calculated distance from the air-fan. This distance was determined by the method discussed here: as the distance of nozzle from air fan was increased, the filament was not cooled efficiently and acceptable diametrical consistencies were not obtained, on the other hand with decrease in this distance, the nozzle temperature was also observed to decrease on the PID display, which reads temperature of the nozzle through a thermocouple seated in a hole on the brass nozzle. An optimum distance was determined by first shifting the extruder to a position where the nozzle is just above the underlying fixed fan, this caused the PID display to show decreasing nozzle temperature. Then the extruder was gently pushed away from the air fan until the PID display stopped

showing decreasing nozzle temperatures. At this position of extruder nozzle, the PID display shows an almost stable temperature reading (within ±2.5°C).

INFORMATION ABOUT THE AUTHOR

Saket Thapliyal was born in Karnaprayag, a city located in the Himalayan region of India and was raised in Dehradun, India. After earning his bachelor's degree from Mechanical Engineering, Saket moved to Arlington, Texas to pursue Master of Science in Mechanical Engineering from the University of Texas at Arlington. Saket joined the Multiscale Mechanics and Physics Laboratory (MMPL) in May 2016 and started working on manufacturing, characterization and processing of multifunctional nanocomposite materials under the supervision of Dr. Ashfaq Adnan (Associate Professor at the Department of Mechanical and Aerospace Engineering at UTA). His research interests include synthesis and characterization of nano-composites, bioinspired and multifunctional materials for additive manufacturing and advanced fabrication and manufacturing technologies.

(Email correspondence: saket.thapliyal@mavs.uta.edu or saketthapliyal@gmail.com)